*Recruitment of co-repressor proteins and histone deacetylation on the MS4A1 promoter in the absence of epigenetic drugs*

To study the molecular mechanisms of transcriptional repression of *MS4A1*, a ChIP assay was performed. RRBL1 cells were incubated with or without 5-Aza-dC and TSA, and a ChIP assay was carried out using anti-Pu.1, -IRF4, -Sin3A, -HDAC1, and -acetylated-histone H4 antibodies. After IP, precipitated genomic DNA was utilized in semi-quantitative PCR using primers for the *MS4A1* promoter (Fig. 3A) and the 3′-intron sequences as a negative control. IRF4 and Pu.1 interactions were consistently observed on the promoter region, but not on the 3′-intron region (Fig. 3B, lanes 5–8). Sin3A and HDAC1, which form a transcription repressor protein complex [26], interacted with the promoter region only in the absence of 5-Aza-dC and TSA (Fig. 3B, lanes 11 and 13). Acetylated-histone H4 was observed at the promoter region with 5-Aza-dC and TSA, but the acetylation was decreased in the absence of the two drugs (lane 9). In the 3′-intron region, histone acetylation was consistently observed with or without 5-Aza-dC and TSA. These results strongly suggest that the Sin3A–HDAC1 co-repressor complex may be recruited to the *MS4A1* promoter through some transcription factors in the absence of epigenetic drugs, resulting in histone deacetylation and transcriptional repression. In addition, the recruitment may be dissociated from the promoter by adding 5-Aza-dC and TSA, resulting in histone acetylation and transcription activation.

*The Sin3A–HDAC1 co-repressor complex is found in RRBL1 cells with or without epigenetic drugs*

To show that loss of Sin3A–HDAC1 interaction with the *MS4A1* promoter was due to protein complex dissociation and not degradation, we confirmed the protein expression in RRBL1 cells with and without epigenetic drugs using IB. As shown in Fig. 4A, HDAC1 and Sin3A protein expression levels did not change in the presence of epigenetic drugs. Next, we performed an IP assay using anti-IRF4, -Sin3A, and -HDAC1 antibody to confirm that Sin3A and HDAC1 exist as a protein complex, and to examine whether the Sin3A–HDAC1 co-repressor complex was recruited by IRF4 in the absence of epigenetic drugs. The Sin3A–HDAC1 interaction was confirmed with an IP assay using anti-Sin3A and -HDAC1 antibodies (Fig. 4B, lanes 4 and 5), but interaction of IRF4 with this complex was not observed (lane 3). These results indicate that the Sin3A–HDAC1 complex exists in RRBL1 cells with or without 5-Aza-dC and TSA, and that the recruitment of the complex to the *MS4A1* promoter may not involve a direct interaction with IRF4.

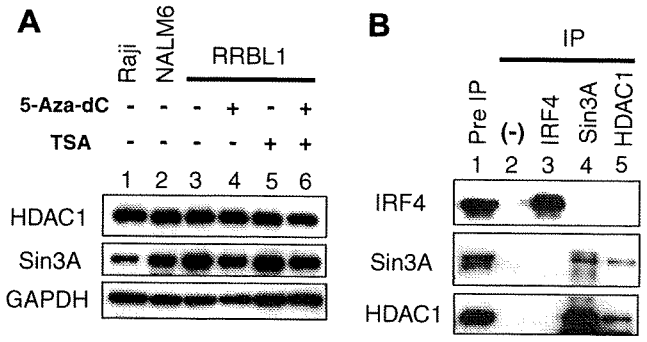


**Fig. 4.** The Sin3A–HDAC1 co-repressor complex is stably expressed in RRBL1 cells with or without 5-Aza-dC and/or TSA. (A) IB was performed using the RRBL1 lysate after treatment with 5-Aza-dC and/or TSA. Raji and NALM6 cells were used as expression controls. Similar levels of expression of HDAC1 and Sin3A were observed in each sample. (B) Whole cell lysate of RRBL1 cells was obtained using lysis buffer. Lysates were divided into four samples and used for IP using anti-IRF4, -Sin3A, and -HDAC1 antibodies. Five percent of the whole cell lysate was used for the pre-IP samples (lane 1). As a negative control, antibodies for IP were omitted (lane 2). IB indicated that endogenous Sin3A–HDAC1 interacted in RRBL1 cells without epigenetic drugs, but significant interaction with IRF4 was not observed in this assay system.

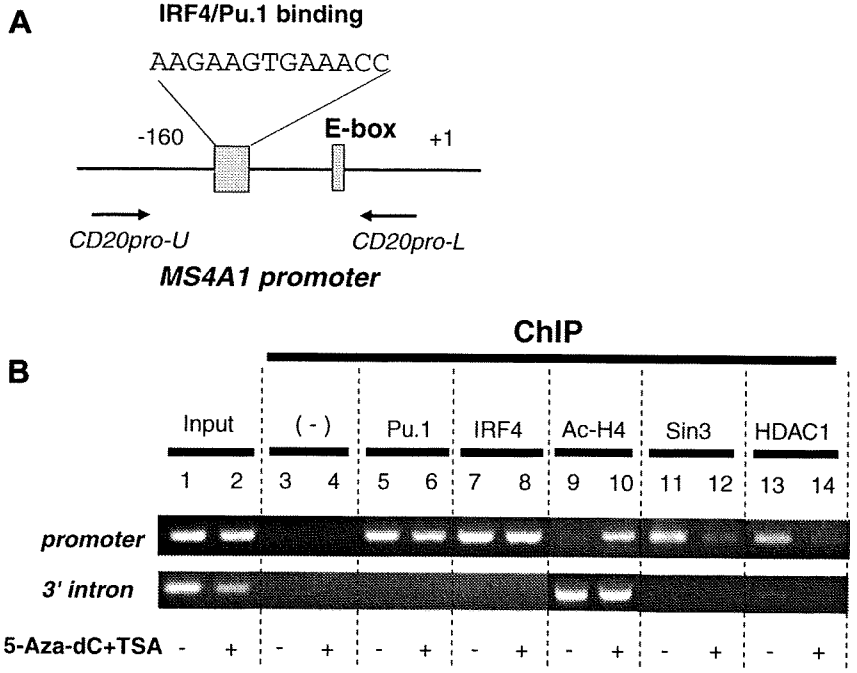


**Fig. 3.** ChIP assay of the *MS4A1* promoter. The primer set used for amplification of the *MS4A1* promoter (−160 to +1) is shown in (A). The positions of the upper and lower primers are indicated as black arrows. (B) A ChIP assay using anti-Pu.1, -IRF4, -Sin3A, -HDAC1, and -acetylated-histone H4 was performed using the cell lysate from cells treated with or without 5-Aza-dC and TSA. Semi-quantitative PCR was performed, and the amplified DNA fragments were visualized by 1.5% agarose gel electrophoresis. As a positive control, lysate without the IP step was used (input). A ChIP sample without antibodies was used as a negative control (−). PCR using the primers for the 3′-intron region of *MS4A1* was also used as a control. Sin3A and HDAC1 recruitment to the promoter was observed in lanes 11 and 13, and accumulation of histone deacetylation was seen in lane 9.

## Discussion

In clinical practice, CD20 expression abnormalities have been reported. Johnson et al. [18] reported that 43 out of 272 (16%) patients with diffuse large B-cell lymphoma (DLBCL) showed reduced CD20 expression using FCM analysis at the time of initial diagnosis, and that the survival rate of this phenotype was significantly lower than that of patients with CD20-positive phenotype. Furthermore, we previously reported that a CD20-negative phenotypic change after using rituximab resulted in resistance to salvage chemotherapies with or without rituximab [6,7]. We observed that all of these patients died of disease progression within 1 year after the diagnosis of CD20-negative transformation, suggesting that the CD20-negative phenotype may be related to the poor prognosis. From these findings, we realized the importance of investigating the mechanisms of downmodulation of CD20 expression to explore overcoming strategies including salvage combination chemotherapies with anti-CD20 antibodies.

In this study, we firstly investigated the effect of 5-Aza-dC on RRBL1 cells. DNMT1 protein reduction was observed 1 day after adding 5-Aza-dC, followed by temporal upregulation of CD20 protein expression (Fig. 1B). This phenomenon suggested that CpG demethylation of the *MS4A1* promoter region was a result of DNMT1 depletion. But interestingly, significant CpG islands were not located at the promoter, suggesting that *MS4A1* activation by 5-Aza-dC was not regulated directly by *MS4A1* promoter methylation.

The next hypothesis we investigated was that expression of transcription factors, which is critical for *MS4A1* expression, was regulated by the methylation status of the promoter DNA. We analyzed the protein expression level of IRF4/Pu.1, and only a modest upregulation was observed. Furthermore, the ChIP assay showed that IRF4/Pu.1 recruitment to the *MS4A1* promoter was fairly stable in the presence or absence of 5-Aza-dC and TSA (Fig. 3B). On the other hand, Sin3A–HDAC1 recruitment and histone deacetylation was observed in the absence of epigenetic drugs. Because previous reports have indicated that HDACs form large protein complexes, such as Sin3 [26], NuRD/Mi-2 [27], and N-CoR/SMRT co-repressor complexes [26,28], and are recruited to the specific promoter by transcription factors, we analyzed whether the Sin3A–HDAC1 complex interacts with IRF4 in RRBL1 cells. Using an IP assay, we observed that HDAC1 interacts with Sin3A but not with IRF4 (Fig. 4B). We also analyzed the recruitment of the proteins N-CoR, HDAC3, and TBLR1 (transducin β-like protein 1 relating protein), which are all expressed in the same co-repressor complex *in vivo* [21–23,26,28], to the promoter region using the ChIP assay. Significant recruitment of these proteins was not seen in this assay (data not shown).

Thus, these findings suggest that, (1) *MS4A1* repression is not directly regulated by methylation of its promoter and (2) transcription factors other than IRF4 recruit the Sin3A–HDAC1 co-repressor complex to the *MS4A1* promoter to repress transcription through histone deacetylation. Our previous report [6] showed that treatment with TSA without 5-Aza-dC upregulates CD20 expression in RRBL1 cells within 1 day, suggesting that the activity of HDAC may be more critical for *MS4A1* expression than the activity of DNMTs. One explanation for why 5-Aza-dC can stimulate *MS4A1* expression is that the expression of some transcription factors, whose expression is critical for CD20 expression, may be regulated by CpG methylation of the gene promoters. The maximal effect of 5-Aza-dC on CD20 protein expression was seen at 3 days after treatment with 5-Aza-dC, which is consistent with this hypothesis. The knockdown of endogenous DNMT1 using the siRNA technique may help explain the importance of DNMT1 for *MS4A1* repression. On the other hand, the possibility that CpG islands in *MS4A1* that affect its expression are in a location that is relatively remote (~5 kb) from the transcription start site cannot be excluded. Further investigation is needed.

In our study, the efficiency of stimulating CD20 protein expression in CD20-negative transformed cells using epigenetic drugs is not complete (Fig. 2B). As we showed previously [7], this efficiency may not be sufficient to overcome resistance to rituximab. Using the newer generation humanized-anti-CD20 monoclonal antibodies, such as ofatumumab [29], GA-101 [30], and others, which have higher antibody binding capacity with CD20 and/or a higher CDC/ADCC activity, may help overcome the resistance. We also anticipate the use of those therapies in combination with epigenetic drugs such as HDAC and/or DNMT inhibitors. Further investigation is still needed.

## Acknowledgments

This work is supported in part by a Grant-in-Aid for Cancer Research (21-6-3) from the Ministry of Health, Labor and Welfare, a Grant-in-Aid from the National Institute of Biomedical Innovation, and a Grant-in-Aid in Scientific Research (20591116) from the Ministry of Education, Culture, Sports, Science and Technology, Japan. We thank Dr. Shinsuke Iida for providing critical information about IRF4. We also thank Akihide Atsumi, Tomoka Wakamatsu, Yukie Konishi, Mari Otsuka, Eriko Ushida, and Chieko Kataoka for valuable laboratory assistance.

## References

[1] B.D. Cheson, Monoclonal antibody therapy for B-cell malignancies, Semin. Oncol. 33 (2006) S2–S14.
[2] B. Coiffier, E. Lepage, J. Briere, R. Herbrecht, H. Tilly, R. Bouabdallah, P. Morel, E. Van Den Neste, G. Salles, P. Gaulard, F. Reyes, P. Lederlin, C. Gisselbrecht, CHOP chemotherapy plus rituximab compared with CHOP alone in elderly patients with diffuse large-B-cell lymphoma, N. Engl. J. Med. 346 (2002) 235–242.
[3] B.D. Cheson, J.P. Leonard, Monoclonal antibody therapy for B-cell non-Hodgkin's lymphoma, N. Engl. J. Med. 359 (2008) 613–626.
[4] M.R. Smith, Rituximab (monoclonal anti-CD20 antibody): mechanisms of action and resistance, Oncogene 22 (2003) 7359–7368.
[5] M.S. Czuczman, S. Olejniczak, A. Gowda, A. Kotowski, A. Binder, H. Kaur, J. Knight, P. Starostik, J. Deans, F.J. Hernandez-Ilizaliturri, Acquirement of rituximab resistance in lymphoma cell lines is associated with both global CD20 gene and protein down-regulation regulated at the pretranscriptional and posttranscriptional levels, Clin. Cancer Res. 14 (2008) 1561–1570.
[6] A. Tomita, J. Hiraga, H. Kiyoi, M. Ninomiya, T. Sugimoto, M. Ito, T. Kinoshita, T. Naoe, Epigenetic regulation of CD20 protein expression in a novel B-cell lymphoma cell line, RRBL1, established from a patient treated repeatedly with rituximab-containing chemotherapy, Int. J. Hematol. 86 (2007) 49–57.
[7] J. Hiraga, A. Tomita, T. Sugimoto, K. Shimada, M. Ito, S. Nakamura, H. Kiyoi, T. Kinoshita, T. Naoe, Down-regulation of CD20 expression in B-cell lymphoma cells after treatment with rituximab-containing combination chemotherapies: its prevalence and clinical significance, Blood 113 (2009) 4885–4893.
[8] T. Sonoki, Y. Li, S. Miyanishi, H. Nakamine, N. Hanaoka, H. Matsuoka, I. Mori, H. Nakakuma, Establishment of a novel CD20 negative mature B-cell line, WILL2, from a CD20 positive diffuse large B-cell lymphoma patient treated with rituximab, Int. J. Hematol. 89 (2009) 400–402.
[9] I. Jilani, S. O'Brien, T. Manshuri, D.A. Thomas, V.A. Thomazy, M. Imam, S. Naeem, S. Verstovsek, H. Kantarjian, F. Giles, M. Keating, M. Albitar, Transient down-modulation of CD20 by rituximab in patients with chronic lymphocytic leukemia, Blood 102 (2003) 3514–3520.
[10] T. Kinoshita, H. Nagai, T. Murate, H. Saito, CD20-negative relapse in B-cell lymphoma after treatment with rituximab, J. Clin. Oncol. 16 (1998) 3916.
[11] T.A. Davis, D.K. Czerwinski, R. Levy, Therapy of B-cell lymphoma with anti-CD20 antibodies can result in the loss of CD20 antigen expression, Clin. Cancer Res. 5 (1999) 611–615.
[12] A.J. Ferreri, G.P. Dognini, C. Verona, C. Patriarca, C. Doglioni, M. Ponzoni, Re-occurrence of the CD20 molecule expression subsequent to CD20-negative relapse in diffuse large B-cell lymphoma, Haematologica 92 (2007) e1–e2.
[13] Y. Terui, Y. Mishima, N. Sugimura, K. Kojima, T. Sakurai, R. Kuniyoshi, A. Taniyama, M. Yokoyama, S. Sakajiri, K. Takeuchi, C. Watanabe, S. Takahashi, Y. Ito, K. Hatake, Identification of CD20 C-terminal deletion mutations associated with loss of CD20 expression in non-Hodgkin's lymphoma, Clin. Cancer Res. 15 (2009) 2523–2530.
[14] R. Lapalombella, B. Yu, G. Triantafillou, Q. Liu, J.P. Butchar, G. Lozanski, A. Ramanunni, L.L. Smith, W. Blum, L. Andritsos, D.S. Wang, A. Lehman, C.S. Chen, A.J. Johnson, G. Marcucci, R.J. Lee, L.J. Lee, S. Tridandapani, N. Muthusamy, J.C. Byrd, Lenalidomide down-regulates the CD20 antigen and antagonizes direct and antibody-dependent cellular cytotoxicity of rituximab on primary chronic lymphocytic leukemia cells, Blood (2008).

[15] A.R. Jazirehi, M.I. Vega, B. Bonavida, Development of rituximab-resistant lymphoma clones with altered cell signaling and cross-resistance to chemotherapy, Cancer Res. 67 (2007) 1270–1281.
[16] B. Bonavida, Rituximab-induced inhibition of antiapoptotic cell survival pathways: implications in chemo/immunoresistance, rituximab unresponsiveness, prognostic and novel therapeutic interventions, Oncogene 26 (2007) 3629–3636.
[17] T. van Meerten, R.S. van Rijn, S. Hol, A. Hagenbeek, S.B. Ebeling, Complement-induced cell death by rituximab depends on CD20 expression level and acts complementary to antibody-dependent cellular cytotoxicity, Clin. Cancer Res. 12 (2006) 4027–4035.
[18] N.A. Johnson, M. Boyle, A. Bashashati, S. Leach, A. Brooks-Wilson, L.H. Sehn, M. Chhanabhai, R.R. Brinkman, J.M. Connors, A.P. Weng, R.D. Gascoyne, Diffuse large B-cell lymphoma: reduced CD20 expression is associated with an inferior survival, Blood 113 (2009) 3773–3780.
[19] G. Egger, G. Liang, A. Aparicio, P.A. Jones, Epigenetics in human disease and prospects for epigenetic therapy, Nature 429 (2004) 457–463.
[20] C.B. Yoo, P.A. Jones, Epigenetic therapy of cancer: past, present and future, Nat. Rev. Drug Discov. 5 (2006) 37–50.
[21] A. Tomita, D.R. Buchholz, Y.B. Shi, Recruitment of N-CoR/SMRT-TBLR1 corepressor complex by unliganded thyroid hormone receptor for gene repression during frog development, Mol. Cell. Biol. 24 (2004) 3337–3346.
[22] A. Atsumi, A. Tomita, H. Kiyoi, T. Naoe, Histone deacetylase 3 (HDAC3) is recruited to target promoters by PML-RARalpha as a component of the N-CoR co-repressor complex to repress transcription in vivo, Biochem. Biophys. Res. Commun. 345 (2006) 1471–1480.
[23] A. Tomita, D.R. Buchholz, K. Obata, Y.B. Shi, Fusion protein of retinoic acid receptor alpha with promyelocytic leukemia protein or promyelocytic leukemia zinc finger protein recruits N-CoR-TBLR1 corepressor complex to repress transcription in vivo, J. Biol. Chem. 278 (2003) 30788–30795.
[24] K. Ghoshal, J. Datta, S. Majumder, S. Bai, H. Kutay, T. Motiwala, S.T. Jacob, 5-Aza-deoxycytidine induces selective degradation of DNA methyltransferase 1 by a proteasomal pathway that requires the KEN box, bromo-adjacent homology domain, and nuclear localization signal, Mol. Cell. Biol. 25 (2005) 4727–4741.
[25] A. Himmelmann, A. Riva, G.L. Wilson, B.P. Lucas, C. Thevenin, J.H. Kehrl, PU.1/Pip and basic helix loop helix zipper transcription factors interact with binding sites in the CD20 promoter to help confer lineage- and stage-specific expression of CD20 in B lymphocytes, Blood 90 (1997) 3984–3995.
[26] M.G. Rosenfeld, V.V. Lunyak, C.K. Glass, Sensors and signals: a coactivator/corepressor/epigenetic code for integrating signal-dependent programs of transcriptional response, Genes Dev. 20 (2006) 1405–1428.
[27] S.A. Denslow, P.A. Wade, The human Mi-2/NuRD complex and gene regulation, Oncogene 26 (2007) 5433–5438.
[28] J. Li, J. Wang, Z. Nawaz, J.M. Liu, J. Qin, J. Wong, Both corepressor proteins SMRT and N-CoR exist in large protein complexes containing HDAC3, EMBO J. 19 (2000) 4342–4350.
[29] A. Hagenbeek, O. Gadeberg, P. Johnson, L.M. Pedersen, J. Walewski, A. Hellmann, B.K. Link, T. Robak, M. Wojtukiewicz, M. Pfreundschuh, M. Kneba, A. Engert, P. Sonneveld, M. Flensburg, J. Petersen, N. Losic, J. Radford, First clinical use of ofatumumab, a novel fully human anti-CD20 monoclonal antibody in relapsed or refractory follicular lymphoma: results of a phase 1/2 trial, Blood 111 (2008) 5486–5495.
[30] T. Robak, GA-101, a third-generation, humanized and glyco-engineered anti-CD20 mAb for the treatment of B-cell lymphoid malignancies, Curr. Opin. Investig. Drugs 10 (2009) 588–596.

# KW-2449, a novel multikinase inhibitor, suppresses the growth of leukemia cells with FLT3 mutations or T315I-mutated *BCR/ABL* translocation

*Yukimasa Shiotsu,[1] *Hitoshi Kiyoi,[2] Yuichi Ishikawa,[2,3] Ryohei Tanizaki,[3] Makiko Shimizu,[1] Hiroshi Umehara,[1] Kenichi Ishii,[1] Yumiko Mori,[2,3] Kazutaka Ozeki,[2] Yosuke Minami,[3] Akihiro Abe,[3] Hiroshi Maeda,[4] Tadakazu Akiyama,[1] Yutaka Kanda,[1] Yuko Sato,[5] Shiro Akinaga,[4] and Tomoki Naoe[3]

[1]Fuji Research Park, Kyowa Hakko Kirin, Shizuoka; [2]Department of Infectious Diseases and [3]Department of Hematology and Oncology, Nagoya University Graduate School of Medicine, Nagoya; [4]Clinical Development Division, Kyowa Hakko Kirin, Tokyo; and [5]Research Institute, International Medical Center of Japan, Tokyo, Japan

**KW-2449, a multikinase inhibitor of FLT3, ABL, ABL-T315I, and Aurora kinase, is under investigation to treat leukemia patients. In this study, we examined its possible modes of action for antileukemic effects on FLT3-activated, FLT3 wild-type, or imatinib-resistant leukemia cells. KW-2449 showed the potent growth inhibitory effects on leukemia cells with FLT3 mutations by inhibition of the FLT3 kinase, resulting in the down-regulation of phosphorylated-FLT3/STAT5, $G_1$ arrest, and apoptosis. Oral administration of KW-2449 showed dose-dependent and significant tumor growth inhibition in FLT3-mutated xenograft model with minimum bone marrow suppression. In FLT3 wild-type human leukemia, it induced the reduction of phosphorylated histone H3, $G_2$/M arrest, and apoptosis. In imatinib-resistant leukemia, KW-2449 contributed to release of the resistance by the simultaneous down-regulation of BCR/ABL and Aurora kinases. Furthermore, the antiproliferative activity of KW-2449 was confirmed in primary samples from AML and imatinib-resistant patients. The inhibitory activity of KW-2449 is not affected by the presence of human plasma protein, such as α1-acid glycoprotein. These results indicate KW-2449 has potent growth inhibitory activity against various types of leukemia by several mechanisms of action. Our studies indicate KW-2449 has significant activity and warrants clinical study in leukemia patients with FLT3 mutations as well as imatinib-resistant mutations. (Blood. 2009;114:1607-1617)**

## Introduction

Overexpression and activating mutations of protein tyrosine kinases (PTK) are frequently observed in several kinds of hematologic malignancies.[1,2] Abnormally activated PTK-mediated signal transduction pathways are involved in their pathogenesis, such as autonomous proliferation, antiapoptosis, and differentiation block. The remarkable clinical success of the ABL kinase inhibitor, imatinib mesylate (IM), in the treatment of BCR/ABL-positive chronic myeloid leukemia (CML) and acute lymphoblastic leukemia (ALL) has proved the principle of molecularly targeted therapy.[3,4] Therapeutic intervention targeting PTKs is therefore highly expected to improve prognosis of patients with hematologic malignancy. FMS-like receptor tyrosine kinase (FLT3) is a class III receptor tyrosine kinase together with cKIT, FMS, and PDGFR.[5,6] FLT3 mutations were first reported as internal tandem duplication (FLT3/ITD) of the juxtamembrane domain-coding sequence; subsequently, a missense point mutation at the Asp835 residue and point mutations, deletions, and insertions in the codons surrounding Asp835 within a tyrosine kinase domain of FLT3 (FLT3/KDM) have been found.[7,8] FLT3 mutation is the most frequent genetic alteration in acute myeloid leukemia (AML) and involved in the signaling pathway of proliferation and survival in leukemia cells.[5,6] Several large-scale studies have confirmed that FLT3/ITD is strongly associated with leukocytosis and a poor prognosis.[9] In addition to FLT3 mutation, overexpression of FLT3 is an unfavorable prognostic factor for overall survival in AML, and it has been revealed that overexpressed FLT3 had the same sensitivity to the FLT3 inhibitor as FLT3/ITD.[10] Because high-dose chemotherapy and stem cell transplantation cannot conquer the adverse effects of FLT3 mutations, it is expected that the development of FLT3 kinase inhibitors will make more efficacious therapeutic strategy for leukemia therapy.[11,12] To date, several small-molecule tyrosine kinase inhibitors have been shown to have a potency to inhibit the FLT3 kinase, and several of them, such as CEP-701, PKC412, MLN-518, and SU11248, have been subjected to clinical trials.[13-16] However, the clinical efficacy of these FLT3 inhibitors for AML with FLT3 mutations is limited to the transient clearance of leukemia blast cells as a single agent; thus, the therapeutic strategy of some FLT3 inhibitors moves toward a combination with conventional chemotherapy.[17] This move is a logical step based on the in vitro evidence of the synergy with conventional cytotoxic agents,[18,19] although it should be considered that several problems regarding adverse effects and pharmacokinetics have been apparent from clinical trials of monotherapy.[20] Furthermore, because acute leukemia is a complex multigenetic disorder,[21-23] a simultaneous inhibition of multiple protein kinases is thought to be advantageous over the increasing potency against the selective kinases. Recent high-throughput resequencing of TK in AML samples revealed new somatic mutations of JAK1, DDR1, and NRTK1 in addition to

Submitted January 13, 2009; accepted May 28, 2009. Prepublished online as *Blood* First Edition paper, June 18, 2009; DOI 10.1182/blood-2009-01-199307.

*Y. Shiotsu and H.K. contributed equally to this study.

The publication costs of this article were defrayed in part by page charge payment. Therefore, and solely to indicate this fact, this article is hereby marked "advertisement" in accordance with 18 USC section 1734.

previously well-known FLT3, cKit, JAK2, and FGFR mutations.[24,25] These observations collectively indicate that FLT3 inhibitors in the next generation should have an adequately balanced potency against key oncogenic kinases, which are responsible for the disease progression and/or the resistance to standard therapeutics. Here we describe efficacy of a novel small-molecule protein kinase inhibitor, KW-2449, which has a potent and unique kinase inhibition profile against FLT3, ABL, T315I-mutant ABL (ABL-T315I) tyrosine kinases as well as Aurora kinase.

## Methods

### Kinase inhibition profile

The in vitro kinase assays were performed according to the KinaseProfiler Assay Protocols of Upstate Biotechnology.

### Growth inhibition profile cell-cycle analysis

FLT3/ITD-, FLT3/D835Y-expressing, wt-FLT3/FL-coexpressing, and FLT3/ITD-green fluorescent protein (GFP)–expressing murine myeloid-progenitor 32D cells were previously reported.[26] Human leukemia cell line MOLM-13 was obtained from DSMZ (German Resource Center for Biological Material); MV4;11, RS4;11, K562, and HL60 from ATCC. Wt-BCR/ABL-positive human ALL cell line TCC-Y and its IM-resistant clones, TCC-Y/sr cells, which has the T315I-mutated BCR/ABL, were reported previously.[27] Cell viability was determined by the sodium 3′-[1-(phenylaminocarbonyl)-3, 4-tetrazolium]-bis (4-methoxy-6-nitro) benzene sulfonic acid hydrate assay after incubation with or without KW-2449 for 72 hours at 37°C. The number of viable cells was determined using the Cell Proliferation Kit II (Roche Diagnostics). For cell-cycle analysis, MOLM-13 and RS4;11 cells were treated with KW-2449. After 24, 48, and 72 hours of incubation at 37°C, DNA contents were analyzed as previously described.[28] Cell cycle distribution of K562, TCC-Y, and TCC/Ysr was analyzed 24 hours after treatment with KW-2449 or imatinib.

### Effects of hAGP on growth inhibitory activity by FLT3 inhibitors

MOLM-13 cells were incubated with various concentrations of KW-2449, PKC-412, and CEP-701 in the presence of 0.1% of human α1-acid glycoprotein (hAGP; Sigma-Aldrich). Cell viability was determined by sodium 3′-[1-(phenylaminocarbonyl)-3, 4-tetrazolium]-bis (4-methoxy-6-nitro) benzene sulfonic acid hydrate assay after incubation for 72 hours at 37°C.

### Western blot

MOLM-13 cells were treated with KW-2449 for 24 hours, and cell pellets were suspended with lysis buffer. FLT3 proteins were immunoprecipitated with anti-FLT3 antibody (S18; Santa Cruz Biotechnology). The precipitated samples were separated by sodium dodecyl sulfate–polyacrylamide gel electrophoresis (SDS-PAGE), and electroblotted onto Immobilon polyvinylidene difluoride membranes (Millipore). Immunoblotting was performed with antiphosphotyrosine antibody (4G10; Upstate Biotechnology). The membranes were incubated with the stripping buffer and then reprobed with anti-FLT3 antibody (C20; Santa Cruz Biotechnology). Signals were developed using an enhanced chemiluminescence system (GE Healthcare). To examine the phosphorylation level of STAT5, whole cell lysates were subjected to immunoblotting with antiphospho-STAT5 antibody (Kyowa Hakko Kogyo). The membranes were incubated with the stripping buffer and then reprobed with anti-STAT5 antibody (Santa Cruz Biotechnology).

RS4;11 cells were suspended in culture medium containing nocodazole with or without KW-2449. After a 30-minute incubation, cells were harvested and cell pellets were suspended in lysis buffer. Whole cell lysates were subjected to immunoblotting with antiphospho-HH3 (Ser10) antibody (Upstate Biotechnology). The membranes were incubated with the stripping buffer and then reprobed with anti-HH3 antibody (Cell Signaling).

### Concentration of KW-2449 in plasma and tumors

Severe combined immunodeficiency (SCID) mice (Fox CHASE C.B-17/Icr-scidJcl, male, 5 weeks old) were purchased from CLEA Japan. Mice were treated with an intraperitoneal injection of antiasialo GM1 antibody (0.3 mg/mouse, Wako Pure Chemical Industries). The day after antiasialo GM1 antibody treatment, all mice were subcutaneously inoculated in the shaved area with $10^7$ of MOLM-13 cells. Ten days after inoculation, KW-2449 at 20 mg/kg was orally administered to mice twice. Blood and tumor samples were collected 4, 8, 12, and 24 hours after the second administration. The plasma and tumor samples were analyzed to measure KW-2449 concentration with liquid chromatography–mass spectrometry–mass spectrometry (LC/MS/MS).

### In vivo antileukemia effects on xenograft transplantation

SCID mice were subcutaneously inoculated with MOLM-13 cells. Five days after inoculation, tumor volume was measured using the Antitumor test system II (Human Life). The 25 mice with tumors ranging from 90 to 130 $mm^3$ were selected and randomized using the Antitumor test system II. From the day of randomization, vehicle (0.5 wt/vol% MC400) or KW-2449 (2.5, 5.0, 10, and 20 mg/kg) was orally administered to mice twice a day for 14 days. Tumor volume was measured twice a week during the treatment.

### In vivo antileukemia effects on syngeneic transplantation

C3H/Hej mice were purchased from Charles River Japan. Fifteen C3H/Hej mice were intravenously inoculated with $2 \times 10^6$ of FLT3/ITD-GFP-32D cells and then randomly divided into 3 groups of 5 mice each. On the seventh day after inoculation, peripheral blood (PB) was collected from the mice. From the 10th day after inoculation, mice were treated with KW-2449 at 40 mg/kg (orally) twice a day, cytosine arabinoside (AraC) at 150 mg/kg (intravenously) daily, or vehicle for 4 days. Six hours after the last administration, PB was collected. Total RNA was extracted from each PB sample using a QIAamp RNA Blood Mini Kit (QIAGEN). cDNA was synthesized from each RNA sample using a random primer and Moloney murine leukemia virus reverse transcriptase (Super-Script II; Invitrogen) according to the manufacturer's recommendations. The expression level of the human FLT3 transcript was quantitated using a real-time fluorescence detection method on an ABI Prism 7000 sequence detection system (Applied Biosystems) as previously reported.[10] After the collection of PB, spleens and bone marrow (BM) cells from femora were collected, and the total cell number from each femur was counted using a cell counter. To discriminate the FLT3/ITD-GFP-32D leukemia cells and normal BM cells, all collected cells were subjected to flow cytometry analysis after phycoerythrin-conjugated antihuman FLT3 monoclonal antibody (SF1.340; Immunotech) staining. In this flow cytometry analysis, GFP-positive cells were defined as residual leukemia in the femur. The weight of each collected spleen was measured.

### Primary patient samples

BM samples from patients with AML or CML in blast crisis were subjected to Ficoll-Hypaque (Pharmacia LKB) density gradient centrifugation. All samples were morphologically confirmed to contain more than 90% leukemia cells after centrifugation on May-Grünwald Giemsa-stained cytospin slides, and then cryopreserved in liquid nitrogen before use. Informed consent was obtained from all patients in accordance with the Declaration of Helsinki to use their samples for the present study as well as banking and molecular analysis, and approval was obtained from the ethics committees of Nagoya University and Ogaki Municipal Hospital for this study. Mutations of the FLT3 gene were examined as previously reported.[8] Primary AML cells were incubated with RPMI1640 medium containing 10% fetal calf serum and 0.1 μM KW-2449 for 6 hours, and cell pellets were suspended with lysis buffer. Whole cell lysates were subjected to immunoblotting with antiphospho-FLT3 (Tyr591) (Cell Signaling Technology) and antiphospho-STAT5 antibodies. The membranes were incubated with the stripping buffer and then reprobed with anti-FLT3 (C20; Santa Cruz Biotechnology) and anti-STAT5 antibodies (Santa Cruz Biotechnology).

### Colony formation analysis

Human AML cells ($10^5$ cells) were plated in MethoCult methylcellulose semisolid medium containing human stem cell factor, granulocyte-macrophage colony-stimulating factor (GM-CSF), and interleukin-3 (H4534; Stem Cell Technologies) with or without KW-2449 (0.1 μM) and then incubated at 37°C for 14 days. Colonies with more than 20 cells were scored using an inverted microscope.

Human cord blood (CB) was collected after full-term deliveries with informed consent obtained in accordance with the Declaration of Helsinki and approved by the Review Board of Tokai Cord Blood Bank. Mononuclear cells were collected by the Ficoll-Hypaque (Pharmacia LKB) density gradient centrifugation. CB mononuclear cells ($5 \times 10^4$ cells) were plated in complete MethoCult methylcellulose medium (H4435; Stem Cell Technologies) with an increasing concentration of KW-2449. After 14 days in culture, erythroid burst-forming units (BFU-E), colony-forming unit–granulocyte macrophage (CFU-GM), and colony-forming unit–granulocyte, erythrocyte, monocyte/macrophage, megakaryocyte (CFU-GEMM) colonies were counted.

### Inhibitory effects on BCR/ABL-positive leukemia cells

K562, TCC-Y, and TCC/Ysr cells were incubated with an increasing concentration of KW-2449 or imatinib for 72 hours, and cell pellets were suspended with lysis buffer. Whole cell lysates were subjected to immunoblotting with antiphospho-ABL (Tyr245; Cell Signaling Technology), antiphospho-STAT5, and anti-poly(ADP-ribose) polymerase (PARP; Cell Signaling Technology) antibodies.

Human CML in blast crisis (CML-BC) cells with T315I-mutation were intravenously inoculated into nonobese diabetic (NOD)/SCID mice (CLEA Japan). On the 28th day after the inoculation, engraftment of leukemia cells in each mouse was confirmed by the detection of human CD45-positive cells in PB. On the next day, PB was collected from the leukemia cell-engrafted mice, and then the mice were treated with KW-2449 at 20 mg/kg twice a day, IM at 150 mg/kg daily, or vehicle for 5 days. Twelve hours after the last administration, PB was collected from each mouse. Total RNA was extracted from each PB sample, and cDNA was synthesized from each RNA sample using a random primer and Moloney murine leukemia virus reverse transcriptase as described in "In vivo antileukemia effects on syngeneic transplantation." The expression level of the BCR/ABL transcript was quantitated using a real-time fluorescence detection method as previously reported.[29] The *GAPDH* served as a control for cDNA quality. Relative gene expression levels were calculated using standard curves and adjusted based on the expression level of the *GAPDH* gene.

After the collection of PB, femora were subjected to pathologic examination. Residual leukemia cells were evaluated by the immunohistochemical staining with antihuman CD45 antibody (Dako North America) as previously reported.[30] The animal experiments were approved by the institutional ethics committee for Laboratory Animal Research, Nagoya University School of Medicine and performed according to the guidelines of the institute.

### Statistical analysis

Differences in continuous variables were analyzed with the Mann-Whitney U test for distribution among 2 groups or the Bonferroni test for distribution among more than 3 groups. Differences in therapeutic effects were analyzed with the repeated-measures analysis of variance method. These statistical analyses were performed with the StatView-J 5.0 software (Abacus Concepts).

## Results

### Development of KW-2449 and its kinase inhibition profile

Our aim was to generate an orally available and highly potent FLT3 inhibitor with low toxicity profile for leukemia patients. For this goal, we screened the chemical libraries of Kyowa Hakko Kirin (previously Kyowa Hakko Kogyo) using several leukemia cells, which have several activated mutations in FLT3 or BCR-ABL translocation. As a result, we identified several chemo-types with different kinase inhibition profiles, intensively studied the structures of the identified chemo-types to improve the potency and selectivity, and then finally generated KW-2449 (Figure 1A).

KW-2449 inhibited FLT3 and ABL kinases with half-maximal inhibitory concentration ($IC_{50}$) values of 0.0066 and 0.014 μM, respectively. In addition, it potently inhibited ABL-T315I, which is associated with IM resistance, with an $IC_{50}$ value of 0.004 μM. On the other hand, KW-2449 had little effect on PDGFRβ, IGF-1R, EGFR, and various serine/threonine kinases even at a concentration of 1 μM. Among various serine/threonine kinases examined, KW-2449 inhibited Aurora A kinase with $IC_{50}$ of 0.048 μM (Table 1) and Aurora B kinase with the equivalent potency (data not shown).

### In vitro effects of KW-2449 on FLT3 mutated leukemia

In vitro kinase inhibition profile of KW-2449 indicated its extreme potency against FLT3 kinase. We first examined the effects of KW-2449 on several human leukemia cell lines with activated FLT3 and mutant FLT3-transfected cells. Because constitutive activation of FLT3 in leukemia cells is reportedly induced by mutation or coexpression of wild-type FLT3 (wt-FLT3) and FLT3 ligand (FL), we evaluated the growth inhibitory effect on mutant FLT3 (FLT3/ITD or FLT3/D835Y)–expressing and wt-FLT3– and FL-coexpressing (wt-FLT3/FL) murine myeloid-progenitor 32D cells. In addition, we evaluated the efficacy against FLT3/ITD-harboring human AML cell lines, MOLM-13 and MV4;11. Previously, we confirmed that FLT3 kinase is constitutively activated in these cell lines, and FI-700, a FLT3 selective inhibitor, can suppress the growth of mutated FLT3 transfected 32D cells as well as MOLM-13 and MV4;11 cells.[31] As expected, KW-2449 showed growth inhibitory activities against FLT3/ITD-, FLT3/D835Y-, and wt-FLT3/FL-expressing 32D cells, MOLM-13 and MV4;11 with half-maximal growth inhibitory concentration ($GI_{50}$) values of 0.024, 0.046, 0.014, 0.024, and 0.011 μM, respectively (Table 2). These results indicate that KW-2449 has the potent growth inhibitory activities against not only FLT3/ITD-expressing leukemia cells but also FLT3/KDM-activated and wild-type FLT3-overexpressing leukemia cells.

It has been reported that PKC-412 and CEP-701, whose chemical structure contains indolocarbazole, tightly bind to hAGP. Although these compounds have been in clinical investigation as FLT3 inhibitors, the significant reduction of their inhibitory activity caused by tight hAGP binding is in part associated with the limited clinical efficacy despite their long exposure in vivo, as well as the potency in vitro.[32,33] In these circumstances, we selected the compounds whose cellular efficacy was not attenuated by the presence of hAGP. Indeed, an addition of hAGP to culture media reduced the growth inhibitory effect of PKC-412 and CEP-701 more than 100- to 1000-fold, whereas the growth inhibitory activity of KW-2449 was not attenuated by hAGP (Figure 1E).

In accordance with growth inhibitory effect, KW-2449 suppressed the phosphorylations of FLT3 (P-FLT3) and its downstream molecule phospho-STAT5 (P-STAT5) in MOLM-13 cells in a dose-dependent manner (Figure 1B). Furthermore, KW-2449 increased the percentage of cells in the $G_1$ phase of the cell cycle and reciprocally reduced the percentage of cells in the S phase, resulting in the increase of apoptotic cell population (Figure 1C-D). These results indicated that the dephosphorylation of constitutively active FLT3 kinase by KW-2449 induced the $G_1$ arrest to leukemia

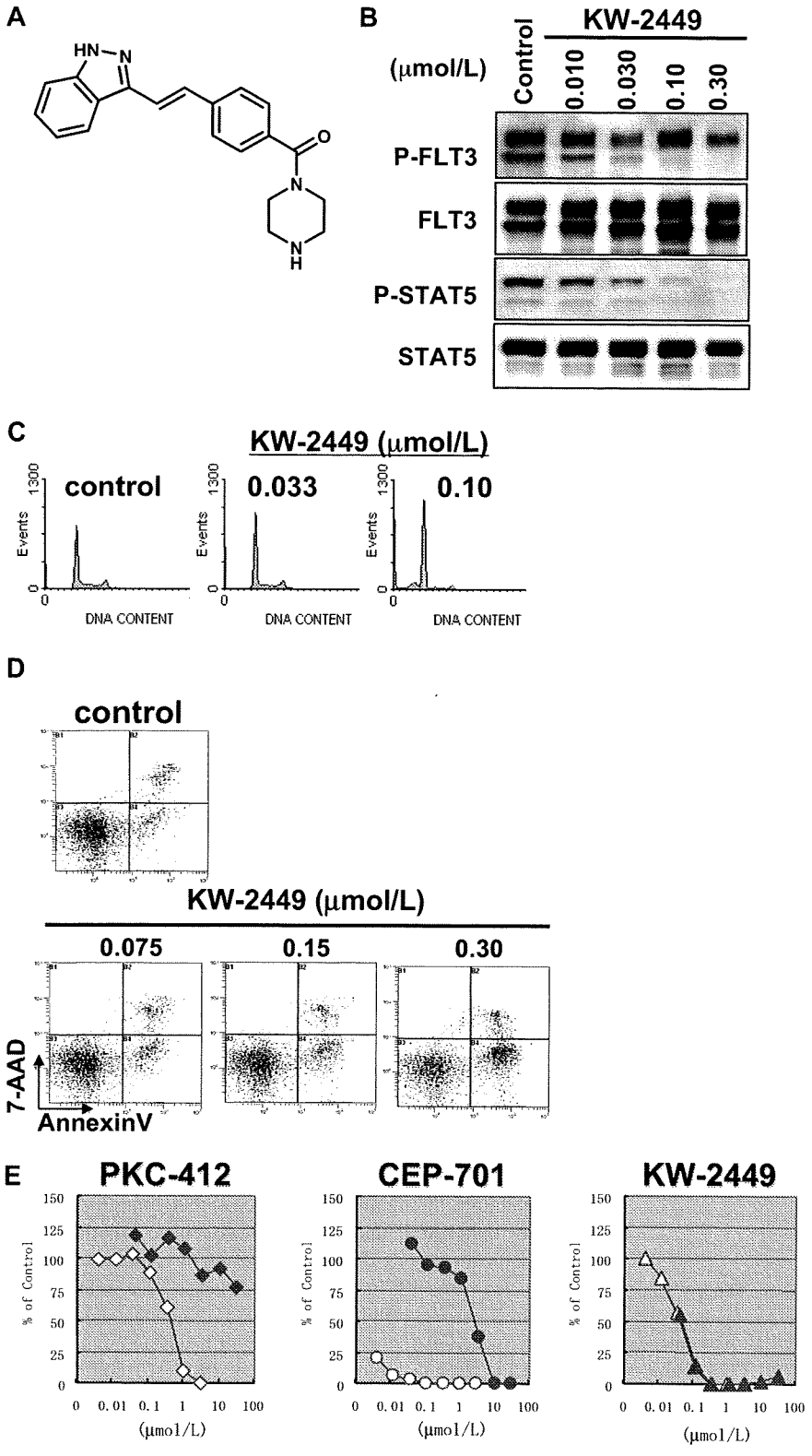


**Figure 1. Effects of KW-2449 on human leukemia cells with FLT3 mutation.** (A) Chemical structure of KW-2449. (B) MOLM-13 cells, which express FLT3/ITD, were treated with KW-2449 at the indicated concentrations for 24 hours. For analysis of FLT3 and its phosphorylated form (P-FLT3), the blots of immunoprecipitated FLT3 SDS-PAGE samples were analyzed by antiphosphotyrosine (P-Tyr) antibody and anti-FLT3 antibody. For detection of STAT5 and its phosphorylated form (P-STAT5), total cell lysate SDS-PAGE samples were analyzed by anti-P-STAT5 antibody and anti-STAT5 antibody as primary antibodies. Phosphorylation levels of FLT3 and STAT5 were decreased by KW-2449 in a dose-dependent manner. (C) MOLM-13 cells were treated with various concentrations of KW-2449 for 48 hours, and cell-cycle distribution was analyzed as described in "Growth inhibition profile and cell-cycle analysis." (D) MOLM-13 cells were treated with various concentrations of KW-2449 for 48 hours, and apoptosis induction was analyzed by 7-amino-actinomycin D/annexin V staining. (E) Inhibitory effects of hAGP on growth inhibitory activity against MOLM-13 cells were compared between KW-2449 and potent FLT3 inhibitors, PKC-412 and CEP-701, as described in "Effects of hAGP on growth inhibitory activity by FLT3 inhibitors." Growth inhibitory activity of KW-2449 was not affected by the presence of hAGP.

cells with FLT3 activation, resulting in apoptosis. Apparent increase of sub-$G_1$ apoptotic cells was also observed after KW-2449 exposure over 0.10 μM, at which concentration complete down-regulation of P-FLT3 was observed.

To confirm these effects on primary leukemia, we further analyzed the activities of KW-2449 using 10 human primary AML cells that consisted of 5 AML with wt-FLT3: 4 with FLT3/ITD and 1 with both FLT3/ITD and FLT3/KDM. In all AML cases with FLT3 mutation, KW-2449 (0.1 μM) reduced the phosphorylation levels both of FLT3 and STAT5 (Figure 2A). In accordance with the dephosphorylation level, the colony formations of AML cases with FLT3 mutation were inhibited by KW-2449 (Figure 2B). In contrast, the inhibitory effect of KW-2449 on the colony formations of all AML cases with wt-FLT3 was minimal at 0.1 μM

**Table 1. Kinase inhibitory profile of KW-2449**

| Kinase | KW-2449 |
|---|---|
| **Tyrosine kinase** | |
| FLT3 | 0.0066 |
| FLT3/D835Y | 0.001 |
| KIT | 0.30 |
| PDGFRα | 1.7 |
| ABL | 0.014 |
| ABL-T315I | 0.004 |
| SRC | 0.40 |
| JAK2 | 0.15 |
| FGFR1 | 0.036 |
| **Serine/threonine kinase** | |
| Aurora A | 0.048 |

In vitro kinase inhibition $IC_{50}$ (μmol/L). $IC_{50}$ values of KW-2449 were determined by in vitro kinase assays as described in "Kinase inhibition profile."

(Figure 2B). In 2 cases with wt-FLT3 (Wt-3 and Wt-5), constitutive phosphorylations of FLT3 were observed, although KW-2449 did not inhibit their colony formations. In the Wt-3 case, the weak inhibitory effect on P-FLT3 might reflect the minimum effect on the colony formation. However, in the Wt-5 case, KW-2449 significantly reduced the level of P-FLT3, whereas the colony formation was not inhibited. In this case, constitutive phosphorylation of STAT5 was also observed, although KW-2449 did not reduce its phosphorylation level, indicating that the STAT5 was phosphorylated by another kinase signal. These results therefore suggested that KW-2449 can dephosphorylate constitutively active wt-FLT3 kinase but not inhibit the proliferation of leukemia cells if they were not mainly addicted to FLT3 the kinase.

The inhibitory effect of KW-2449 on normal hematopoiesis was also evaluated using human hematopoietic progenitors. Mononuclear cells from 5 independent CB were plated in complete methylcellulose semisolid medium with an increasing concentration of KW-2449. Although KW-2449 inhibited the colony formation of CB mononuclear cells in a dose-dependent manner, the distribution of BFU-E, CFU-GM, and CFU-GEMM colonies was not affected by the KW-2449 treatment (Figure 2C-D). The Bonferroni test revealed that statistically significant differences in the total number of colonies were found between control and at the 0.5 μM ($P < .01$) concentration, and at the 0.01 μM and at the 0.5 μM ($P < .05$) concentration. The reduction of a total colony number was at most 59.6% plus or minus 20.2% of the control, at 0.1 μM of KW-2449. These results indicated that the suppressive effect of KW-2449 on the normal hematopiesis was modest, whereas that on leukemia with FLT3 mutations was significant (Figure 2B-C).

**Table 2. Growth inhibitory profile of KW-2449**

| Cell lines | KW-2449 | Imatinib |
|---|---|---|
| **32D transfectant** | | |
| Mock (with IL-3) | > 10 | — |
| FLT3/ITD | 0.024 | — |
| FLT3/D835Y | 0.046 | — |
| Wt-FLT3/FL | 0.014 | — |
| **Human leukemia** | | |
| MOLM-13 | 0.024 | > 10 |
| MV4;11 | 0.011 | — |
| RS4;11 | 0.23 | 20 |
| HL-60 | 0.65 | > 10 |
| **BCR/ABL+ leukemia** | | |
| K562 | 0.27 | 0.24 |
| TCC-Y | 0.49 | 0.18 |
| TCC-Y/sr | 0.42 | 24 |

Growth inhibition $GI_{50}$ (μmol/L). $GI_{50}$ values of KW-2449 and imatinib were determined by in vitro XTT assays. MOLM-13 and MV4;11 cells had FLT3/ITD. K562 and TCC-Y cells had wt-BCR/ABL, and TCC-Y/sr had the T315I mutation in the *BCR/ABL* gene.

— indicates not applicable.

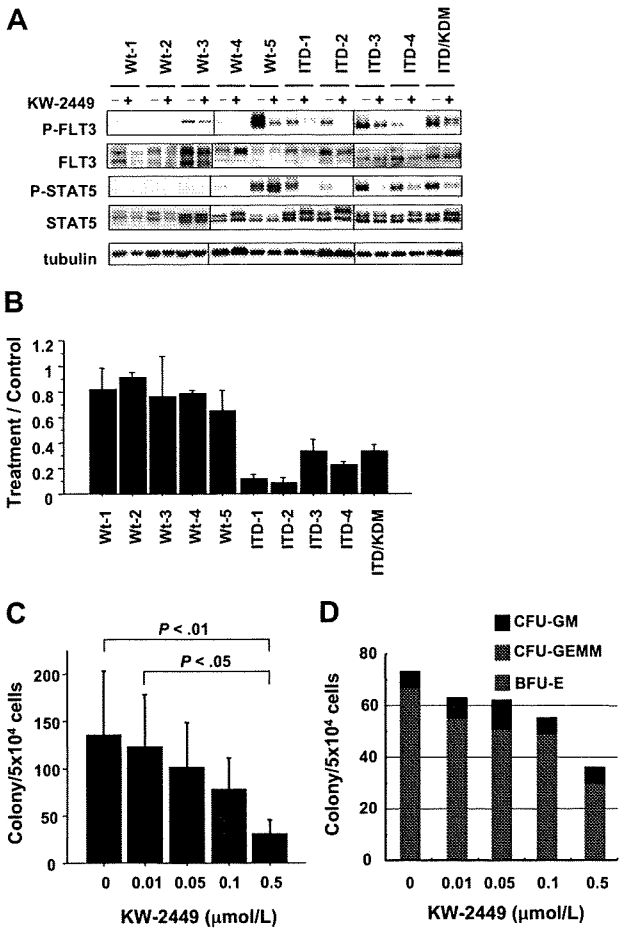


**Figure 2. Inhibitory effects of KW-2449 on primary AML and colony-forming cells.** (A) Ten AML samples consisting of 5 with wild-type FLT3 (Wt-1 to Wt-5), 3 with FLT3/ITD (ITD-1 to ITD-4), and one with both FLT3/ITD and FLT3/KDM (ITD/KDM), were analyzed. Primary AML cells were incubated with or without KW-2449 at 0.1 μM for 6 hours, and then phosphorylation status of FLT3 and STAT5 was analyzed. KW-2449 reduced phosphorylation levels of FLT3 and STAT5 in all AML samples with *FLT3* mutations. In the Wt-5 sample, KW-2449 reduced the phosphorylation level of FLT3 but not of STAT5. Vertical lines have been inserted to indicate a repositioned gel lane. (B) AML cells were suspended in methylcellulose semisolid medium containing human stem cell factor, GM-CSF, and interleukin-3 with or without 0.1 μM KW-2449. Colonies were counted after 14 days. Mean treatment/control ratio ± SD from 3 experiments in each sample are shown. In accordance with the down-regulation levels of FLT3 and STAT5 phosphorylations, KW-2449 inhibited the colony formations in all AML samples with FLT3 mutations. In the Wt-5 sample, weak inhibition of the colony formation seems to reflect the sustained STAT5 activation induced by another activation mechanism. (C) Mononuclear cells from human CB were plated in the complete methylcellulose semisolid medium with an increasing concentration of KW-2449. After 14 days of culture, BFU-E, CFU-GM, and CFU-GEMM colonies were counted. Mean total colony numbers ± SD at the indicated concentrations of KW-2449 are shown (n = 5). Although KW-2449 inhibited a total number of colonies in a dose-dependent manner, the Bonferroni test revealed that the statistical significances were found between control and at the 0.5 μM ($P < .01$), and at the .01 μM and at the 0.5 μM ($P < .05$). (D) The representative result of the distribution of BFU-E, CFU-GM, and CFU-GEMM colonies from 1 CB sample is shown. Although KW-2449 inhibited the colony formation of CB mononuclear cells in a dose-dependent manner, the distribution of BFU-E, CFU-GM, and CFU-GEMM colonies was not affected by the KW-2449 treatment.

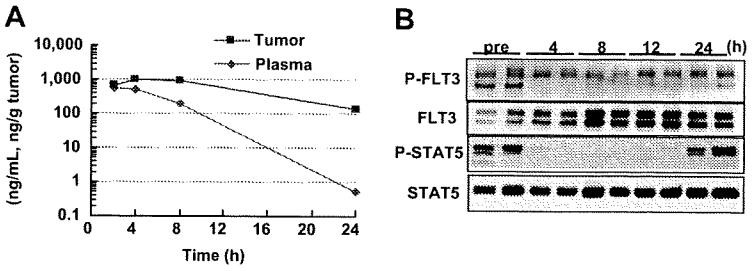


**Figure 3. Pharmacokinetic and pharmacodynamic effects of KW-2449 in FLT3-activated leukemia.** (A) MOLM-13 cells ($10^7$ cells/mouse) were subcutaneously inoculated into 2 SCID mice. Ten days after inoculation, KW-2449 at 20 mg/kg was orally administered twice every 12 hours. The concentrations of KW-2449 in plasma and tumor were sequentially analyzed by LC/MS/MS after the final administration of KW-2449. (B) The transition of FLT3 and STAT5 phosphorylation levels in tumor were analyzed by Western blotting. For analysis of FLT3 and its phosphorylated form (P-FLT3), the blots of immunoprecipitated FLT3 SDS-PAGE samples were analyzed by antiphospho-tyrosine (P-Tyr) antibody and anti-FLT3 antibody. For detection of STAT5 and its phosphorylated form (P-STAT5), total tumor lysate SDS-PAGE samples were analyzed by anti–P-STAT5 antibody and anti-STAT5 antibody as primary antibodies. Dephosphorylations of FLT3 and STAT5 in MOLM-13 were observed until 12 hours after the last administration. Results from 2 mice at each point are shown.

### In vivo effects of KW-2449 on leukemia cells with FLT3 mutation

In vivo antileukemia activities of KW-2449 were evaluated using MOLM-13, FLT3-ITD AML, xenograft model. First, the concentrations of KW-2449 in both plasma and tumor after oral administration were sequentially examined in SCID mice bearing the subcutaneous MOLM-13 tumor. The tumor/plasma concentration ratio of KW-2449 tended to increase along with the time after administration and reached approximately 400, 24 hours after dosing (Figure 3A). The levels of P-FLT3 and P-STAT5 in the tumor were completely reduced from 4 to 12 hours after the administration of KW-2449 (Figure 3B). Although dephosphorylations of FLT3 and STAT5 were observed until 12 hours after administration, these returned to almost the basal level at 24 hours. These results suggested that the oral administration of KW-2449 at a twice daily schedule could be adequate for continuous inhibition of activated FLT3 in the mouse model.

In the MOLM-13 tumor xenograft model, oral administration of KW-2449 for 14 days showed a potent and significant antitumor effect in a dose-dependent manner (Figure 4A). KW-2449 treatment at 2.5 and 5.0 mg/kg twice a day showed growth inhibition of tumors with the ratio of tumor volume in the treated to control mice minimum values ($T/C_{min}$) of 0.57 and 0.29, respectively (Figure 4B). Furthermore, KW-2449 treatment at 10 mg/kg twice a day showed tumor regression with $T/C_{min}$ of 0.010 and treatment at 20 mg/kg twice a day completely eradicated tumors in all mice (Figure 4C).

We next compared the effects of KW-2449 on mutant FLT3-expressing cells with a conventional antileukemic agent, AraC, using the syngeneic transplantation mouse model. Human FLT3/ITD-ires-GFP-expressing 32D (FLT3/ITD-GFP-32D) cells were intravenously inoculated into syngeneic C3H/Hej mice, and then KW-2449, AraC, or vehicle was administered to the mice 11 days after inoculation for 4 days (Figure 5A). At the seventh day after inoculation, mean FLT3 transcript levels in PB were 24.4 plus or minus 6.7, 11.8 plus or minus 5.7, and 42.0 plus or minus 21.7 copies/μg RNA in vehicle-, KW-2449- and AraC-treated mice, respectively. In all vehicle-treated mice, FLT3 transcript level increased, and the mean FLT3 transcript level in PB on day 13 was 5869.6 plus or minus 1640.1 copies/μg RNA. In contrast, KW-2449 treatment repressed the expansion of FLT3/ITD-GFP-32D cells as the decrease of FLT3 transcript levels was observed in all mice, and the mean FLT3 transcript level in PB was 3.25 plus or minus 2.29 copies/μg RNA on day 13. The increase in FLT3 transcripts level in all AraC-treated mice was lower than that in vehicle-treated mice, although the effect of AraC treatment was limited as the mean FLT3 transcript level in PB was 882.7 plus or minus 305.5 copies/μg RNA on day 13. These results demonstrated that the repressive effects by KW-2449 on the expansion of FLT3/ITD-GFP-32D cells were significantly stronger than those by AraC ($P = .026$ by the repeated-measures analysis of variance; Figure 5B). Flow cytometry analysis revealed that KW-2449 significantly eradicated FLT3/ITD-GFP-32D cells from BM (the mean percentages of FLT3/ITD-GFP-32D cells in BM after

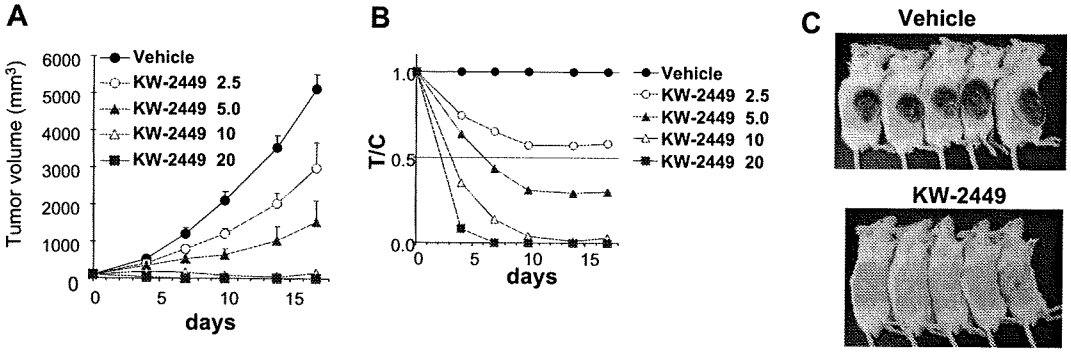


**Figure 4. In vivo efficacy of xenotransplanted tumors with FLT3/ITD.** (A-C) MOLM-13 cells ($10^7$ cells/mouse) were subcutaneously inoculated into SCID mice. Five days after inoculation, tumor volume was measured. The 25 mice with tumors ranging from 90 to 130 $mm^3$ were selected 5 days after inoculation and divided into 5 groups. Mice (n = 5 in each group) were orally administered with vehicle or KW-2449 (2.5, 5.0, 10, and 20 mg/kg) twice a day for 14 days. (A) Tumor volume was measured twice a week during the treatment. Mean tumor volume ± SD is shown. KW-2449 showed potent and significant antitumor effect in a dose-dependent manner. (B) Relative ratio of tumor volume (V) to initial tumor volume (V0) was represented (V/V0). Relative V/V0 ratio of a drug-treated group compared with a control group was represented as T/C. (C) KW-2449 treatment at 20 mg/kg twice a day showed complete regression and disappearance of tumors in all mice.

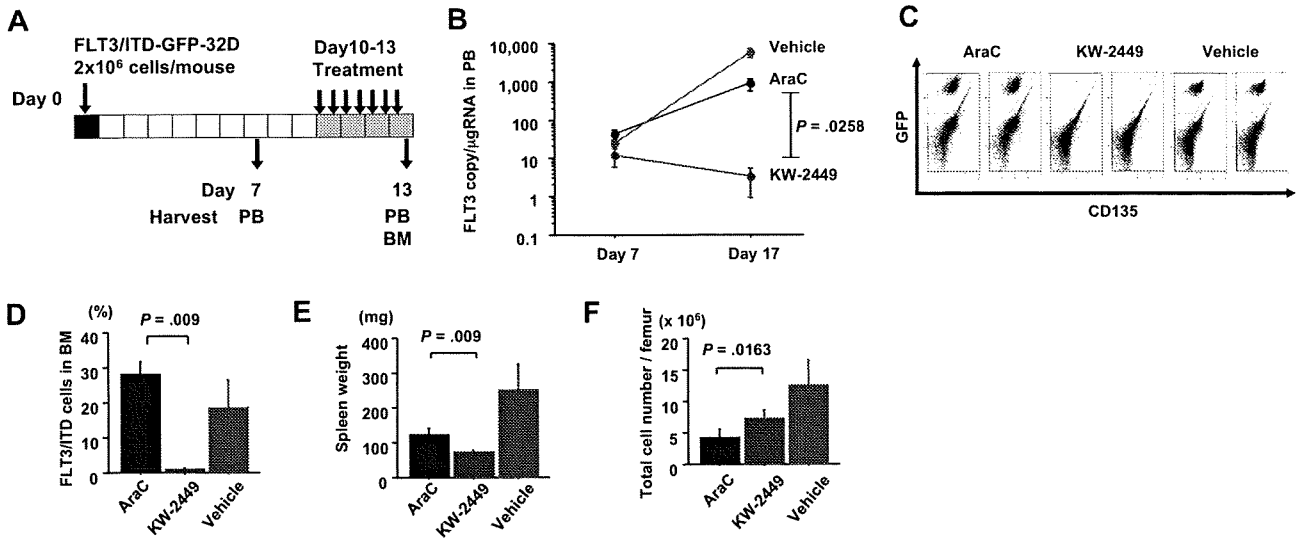


**Figure 5. Inhibition effects on FLT3/ITD-GFP-32D cells in C3H/Hej-mice syngeneic transplantation model.** (A) C3H/Hej mice were inoculated with $2 \times 10^6$ of FLT3/ITD-GFP-32D cells on day 0. From the 10th day after inoculation, mice were administrated with KW-2449 at 40 mg/kg (orally) twice a day, AraC at 150 mg/kg (intravenously) daily or vehicle for 4 days (n = 5 in each group). PB was collected from each mouse on day 7 and day 13. BM was collected on day 13. (B) Human FLT3 transcripts in PB were quantitated by a real-time fluorescence detection method. Mean transcript level ± SEM is shown. KW-2449 treatment significantly repressed the expansion of FLT3/ITD-GFP-32D cells compared with AraC treatment ($P = .026$ by the repeated-measures analysis of variance method). (C) The percentage of residual BM FLT3/ITD-GFP-32D cells in femur was compared among vehicle-, KW-2449-, and AraC-treated mice using flow cytometry. Representative results of flow cytometry are shown. (D) Mean percentages of residual FLT3/ITD-GFP-32D cells plus or minus SD in BM are shown. KW-2449 significantly eradicated FLT3/ITD-GFP-32D cells from BM compared with AraC treatment ($P = .009$ by the Mann-Whitney U test). (E) Mean spleen weight of each treated mouse ± SD is shown. The mean spleen weight of KW-2449-treated mice was significantly lighter than that of AraC-treated mice ($P = .009$ by the Mann-Whitney U test). (F) Mean total cell numbers in femur after the treatment ± SD are shown. The total number of nuclear cells in the BM of AraC-treated mice was significantly decreased compared with that of KW-2449–treated mice ($P = .016$ by the Mann-Whitney U test).

treatment were 30.0% ± 3.6% and 0.75% ± 0.75% in AraC- and KW-2449-treated mice, respectively; $P = .009$ by the Mann-Whitney U test; Figure 5C-D). Furthermore, the mean spleen weight of KW-2449-treated mice was significantly lighter than that of AraC-treated mice (71.4 ± 6.2 and 122.2 ± 20.4 mg, respectively; $P = .009$ by the Mann-Whitney U test; Figure 5E). Notably, the total number of nuclear cells in the BM of AraC-treated mice was significantly decreased compared with that of KW-2449-treated mice ([4.2 ± 1.3] × $10^6$ and [7.3 ± 1.3] × $10^6$ cells/femur, respectively; $P = .016$ by the Mann-Whitney U test; Figure 5F). In this model, we confirmed that KW-2449 could potently and selectively eradicate mutant FLT3-expressing leukemia cells both in PB and BM in contrast to the nonselective BM suppression of conventional cytotoxic agents such as AraC.

### In vitro effects of KW-2449 on FLT3 wild-type leukemia

On the other hand, KW-2449 inhibited the growth of human ALL cell line RS4;11, which expresses unphosphorylated wt-FLT3, with the $GI_{50}$ value of 0.23 μM (Table 2). Because KW-2449 shows potent Aurora A and Aurora B kinase inhibition, we evaluated whether the growth inhibitory effect on RS4;11 was induced by Aurora kinase inhibition. When the cell cycle was arrested in the M-phase by nocodazole, phosphorylated histone-H3 (P-HH3) was clearly observed in RS4;11, but it was decreased by the treatment with KW-2449 in a dose-dependent manner (Figure 6A). Cell cycle distribution analysis indicated that KW-2449 (0.60 μM) induced $G_2$/M arrest and apparent increase of sub-$G_1$ apoptotic cells after 24 hours and 48 hours of exposure, respectively (Figure 6B). Even at 0.30 μM, KW-2449 slightly decreased the population of S-phase cells from 49.0% to 40.6% after 72 hours (histogram data not shown). The increase of annexin V–positive (early apoptotic) cells was also observed at the $GI_{50}$ value against RS4;11 cells (Figure 6C). These results suggested that KW-2449 has a growth inhibitory potency against leukemia cells even without activated FLT3 through the inhibition of Aurora kinase, although its potency was 5- to10-fold lower than that against those with activated FLT3 kinase.

### Effects of KW-2449 on wt and T315I-mutated BCR/ABL-expressing leukemia cells

IM resistance is a critical issue to be resolved in the treatment of patients with BCR/ABL-positive leukemia. Because KW-2449 showed potency against both ABL and ABL-T315I kinases in the in vitro kinase assays, we evaluated its growth inhibitory effects on wt (K562 and TCC-Y) and T315I-mutated (TCC-Y/sr) BCR/ABL-expressing human leukemia cell lines. IM inhibited the growth of K562 and TCC-Y cells with $GI_{50}$ values of 0.24 and 0.18 μM, respectively, whereas its $GI_{50}$ value against TCC-Y/sr was 24 μM, which was approximately 100-fold higher than against K562 and TCC-Y cells. However, KW-2449 equally inhibited the growth of wt and T315I-mutated BCR/ABL-expressing leukemia cells: $GI_{50}$ values were 0.27, 0.49, and 0.42 μM in K562, TCC-Y, and TCC-Y/sr cells, respectively (Table 2). In K562 cells, IM decreased the phosphorylation levels of BCR/ABL and STAT5 (Figure 7A), increased the number of the $G_1$ phase-arrested cells at 0.5 μM, and induced apoptosis, which was also shown by an increase of cleaved PARP (Figure 7A,D). On the other hand, KW-2449 induced $G_2$/M phase-arrested cells at 0.50 μM and increased the sub-$G_1$ and polyploidy cells at 1.0 μM (Figure 7D). These inductions of $G_2$/M arrest and polyploidy in K562 cells are presumed to be caused both by the Aurora A and Aurora B inhibitory profile of KW-2449. In TCC-Y cells, the IM treatment at 0.5 and 1.0 μM decreased the phosphorylation levels of BCR/ABL and STAT5, whereas it did not increase the apoptotic or the $G_1$ phase-arrested cells. In contrast, KW-2449 decreased the phosphorylation levels of BCR/ABL and STAT5 from 0.25 μM and induced the $G_2$/M-arrested cells at

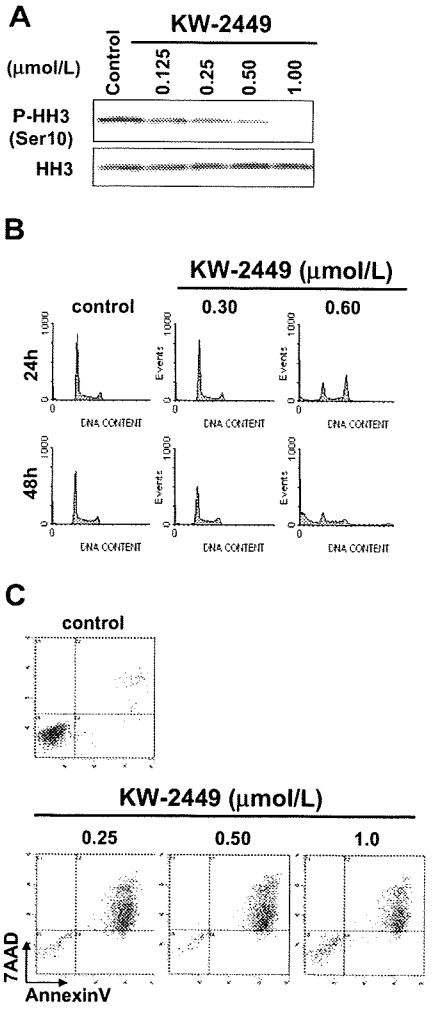


**Figure 6. Effects of KW-2449 on human leukemia cells without FLT3 mutation.** (A) RS4;11 cells, which express wild-type FLT3/ITD, were treated with KW-2449 at the indicated concentrations for 30 minutes. Total and phosphorylation levels of HH3 were analyzed by Western blotting. (B) RS4;11 cells were treated with various concentrations of KW-2449 for 48 hours, and cell-cycle distribution was analyzed. (C) RS4;11 cells were treated with various concentration of KW-2449 for 48 hours, and apoptosis induction was analyzed.

0.25 μM (data not shown), as well as apoptosis at 1.0 μM (Figure 7B,D). In TCC-Y/sr cells, IM did not affect the phosphorylation levels of BCR/ABL and STAT5 as well as apoptosis and the cell cycle, whereas KW-2449 decreased both phosphorylation levels from 0.25 and 0.5 μM, respectively. Furthermore, KW-2449 apparently induced apoptosis at 1.0 μM, which was shown by PARP cleavage and the sub-$G_1$ population (Figure 7C-D).

We next compared the effects of KW-2449 on human CML-BC cells harboring T315I mutation with IM, using the xenotransplantation mouse model. After confirming the engraftment of human CML-BC cells, NOD/SCID mice were administered with KW-2449, IM, or vehicle for 5 days. After the treatment, the BCR/ABL transcript levels in PB increased to 3.391 plus or minus 1.071 and 1.927 plus or minus 0.332 times as much as those before the treatment in the vehicle- and IM-treated mice, respectively. In contrast, KW-2449 significantly decreased BCR/ABL transcript levels as to 0.553 plus or minus 0.288 times as much as those before treatment compared with the vehicle- and IM-treated mice ($P = .001$ and $P = .003$ by the unpaired $t$ test, respectively; Figure 7E). Furthermore, the immunohistochemical analysis showed that KW-2449 dramatically eradicated leukemia cells in BM (Figure 7F). In addition, KW-2449 treatment significantly prolonged the survival time of TCC-Y/sr-inoculated SCID mice (data not shown). These results collectively suggested that KW-2449 potently suppresses the growth both of wt- and T315I-mutated BCR/ABL-expressing leukemia cells by dual-inhibitory activities against BCR/ABL and Aurora kinases.

## Discussion

Here we describe how KW-2449 potently and selectively inhibits the growth of leukemia cells harboring constitutively activated FLT3 kinase both in vitro and in vivo. As described previously, KW-2449 was selected from chemical libraries of Kyowa Hakko Kirin as a highly potent compound whose $GI_{50}$ values against MOLM-13 and FLT3-D835Y-expressing 32D cells were less than 0.10 μM. In parallel, we evaluated the growth inhibitory activities against BCR/ABL-positive K562 cells and several hematologic malignant cell lines. As shown in this study, KW-2449 inhibited FLT3, ABL, and ABL-T315I kinases. In addition to these tyrosine kinases, which are involved in oncogenic addiction of several leukemia cells, KW-2449 has inhibitory effect on Aurora kinase, which is a key regulatory kinase in mitosis. Because KW-2449 potently inhibited the proliferation of various hematologic malignant cells, including wt-BCR/ABL– and T315I-mutated BCR/ABL-expressing cells, with $GI_{50}$ values ranging from 0.014 to 0.65 μM, we evaluated which kinase was targeted in each malignant cell. To address this issue, we analyzed the phosphorylation status of possibly targeted kinases and the cell cycle distribution after KW-2449 treatment. In mutant FLT3-expressing leukemia cells, the reduction of P-FLT3 level was observed from less than 0.030 μM of KW-2449, which was consistent with its growth inhibitory and the $G_1$-arrest effects. In leukemia cells without FLT3 activation such as RS4;11, the sensitivity of KW-2449 was 5- to 10-fold lower than that in mutant FLT3-expressing leukemia cells. In these cells, KW-2449 induced the $G_2$/M arrest or polyploidy and apoptosis at approximately $GI_{50}$ value (0.25 μM) via Aurora kinase inhibition, which was detected by the reduction of P-HH3. It has been reported that P-HH3 is the target molecule of Aurora B kinase, and the decrease of P-HH3 level was observed from 0.125 μM (Figure 6A), whereas $G_2$/M arrest, an indicator of Aurora kinase A inhibition, was clear at 0.60 μM of KW-2449. It suggested that both Aurora B and Aurora A kinase inhibition by KW-2449 contributes antileukemia effects in FLT3 wild-type. These results collectively suggested that KW-2449 potently suppressed the growth of leukemia cells immortalized by FLT3 activation via FLT3 inhibition alone at a lower concentration, whereas the growth suppression of FLT3-inactivated leukemia cells was induced by Aurora inhibition at a higher concentration. It has been reported that several kinase inhibitors, such as MK-0457 (VX-680), simultaneously suppress both FLT3 and Aurora kinases.[34] When we examined the effects of MK-0457 on mutant FLT3-expressing leukemia cells, it induced the $G_2$/M arrest at the $GI_{50}$ values, indicating that its primary cellular target was Aurora kinase, but not FLT3 even in the constitutively FLT3-activated cells (data not shown). However, KW-2449 first inhibits FLT3 kinase with approximately 10-fold higher potency than Aurora kinase. Therefore, this characteristic mode of inhibitory action may be advantageous over the adverse events associated with the Aurora kinase inhibition.

The clinical efficacy of both PKC-412 and CEP-701 given as monotherapy was reportedly unimpressive despite their high

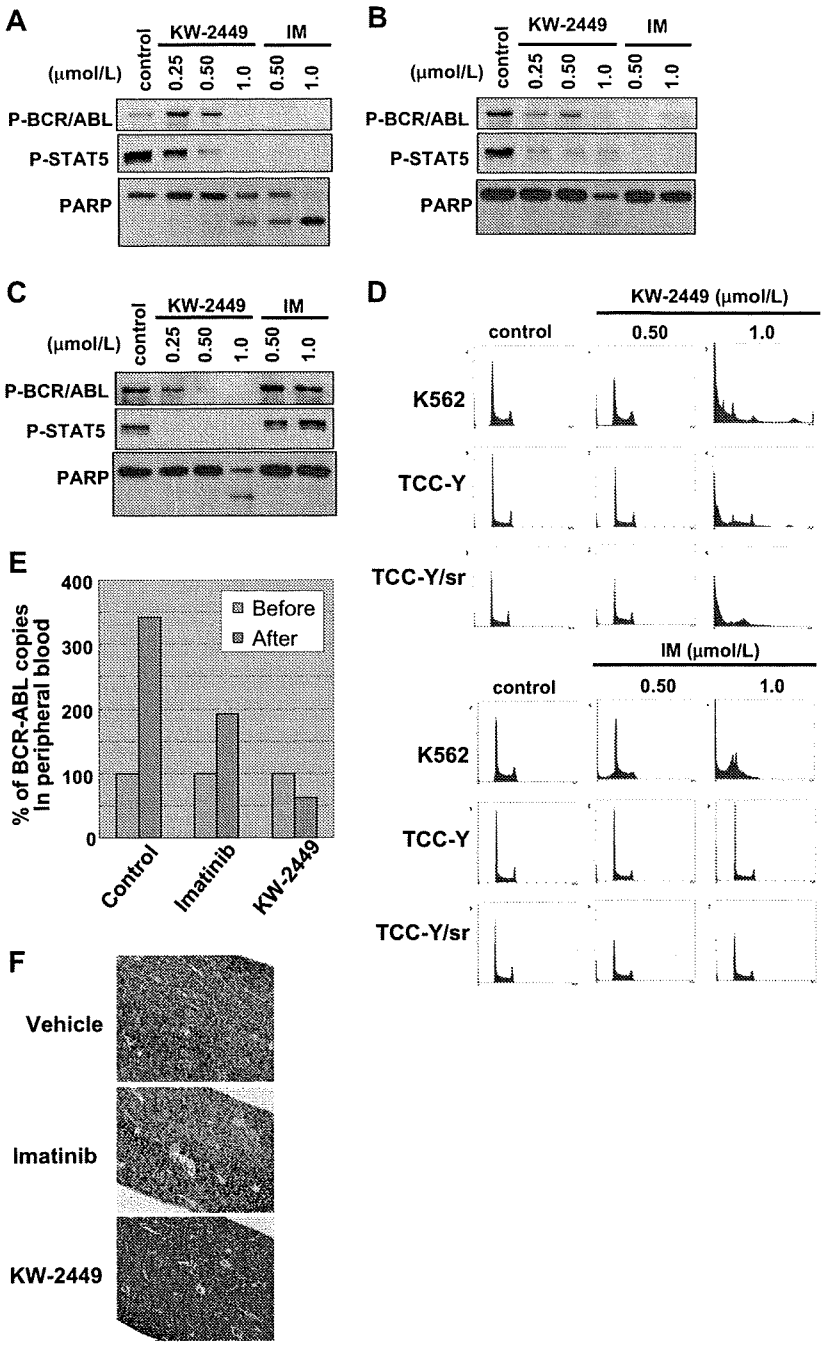


**Figure 7. Inhibitory effects of KW-2449 on BCR/ABL-positive leukemia cells.** We compared inhibitory effects on wt (K562 and TCC-Y) and T315I-mutated (TCC-Y/sr) BCR/ABL-expressing human leukemia cells between KW-2449 and imatinib (IM). (A) In K562 cells, KW-2449 and IM equally decreased the phosphorylation levels of BCR/ABL and STAT5 and increased cleaved PARP. (B) In TCC-Y cells, IM decreased the phosphorylation levels of BCR/ABL and STAT5, but did not increase cleaved PARP. In contrast, KW-2449 decreased the phosphorylation levels of BCR/ABL and STAT5 and increased cleaved PARP. (C) In TCC-Y/sr cells, IM did not affect the phosphorylation levels of BCR/ABL and STAT5, whereas KW-2449 decreased both phosphorylation levels and increased cleaved PARP. (D) DNA contents were also compared between KW-2449 and IM treatments. IM increased the number of the $G_1$-arrested cells only in K562 cells. However, KW-2449 induced the $G_2$/M-arrested cells in K562, TCC-Y, and TCC-Y/sr cells. (E) We compared the antileukemic efficacy in NOD/SCID mice xenotransplanted with human CML in blast crisis cells harboring the T315I mutation after IM treatment. The treatment effects on the leukemia cells in PB are shown by the after/before BCR/ABL transcript ratio. After the treatment, the BCR/ABL transcript levels in PB increased to 3.391 plus or minus 1.071 and 1.927 plus or minus 0.332 times as much as those before the treatment in the vehicle- and IM-treated mice, respectively. In contrast, KW-2449 significantly decreased BCR/ABL transcript levels as to 0.553 ± 0.288 times as much as those before the treatment compared with the vehicle- and IM-treated mice ($P = .001$ and $P = .003$ by the unpaired $t$ test, respectively). (F) Residual leukemia cells in femora were evaluated by the immunohistochemical staining with human CD45. KW-2449 more potently eradicated leukemia cells in BM than IM.

potency in the in vitro studies and extensive exposure in humans. This was partly explained by their structural problem (both compounds are well known as tight binders to hAGP in human plasma) because they contain indolocarbazole motif and result in the significant reduction of their biologic activities in human bodies. In contrast, the growth inhibitory activity of KW-2449 was not attenuated by hAGP, indicating the advantage to keep the biologically active concentration in human plasma.

It is well known that IM that targets the adenosine triphosphate-binding site of the kinase domain of BCR/ABL, inducing remissions in patients with chronic-phase CML. However, whereas responses in the chronic phase were durable, remissions observed in blast crisis patients were typically short-lived, with relapse occurring within 6 months despite continued therapy. Thus, IM resistance is becoming an increasingly recognized problem for the treatment of patients with BCR/ABL-positive leukemia. Several IM-resistant mechanisms, such as acquired mutation in the *BCR/ABL* gene, overexpression of BCR/ABL, hAGP binding, and the emerging other kinase activations, have been reported.[35] To overcome the resistance, ABL kinase inhibitors in the second generation have been investigated, and some of them showed significant clinical response to IM-resistant or refractory patients, although the resistance of T315I-mutated BCR/ABL kinase remains to be resolved.[36] We therefore evaluated the efficacy of KW-2449 for leukemia cells with T315I-mutated BCR/ABL both in vitro and in vivo. KW-2449 at 0.25 μM showed the decrease of P-ABL and P-STAT5 in K562, TCC-Y, and TCC-Y/sr cells, whereas IM had little effect on these signaling molecules in T315I-mutated leukemia (Figure 7A). In addition to inhibitory activity of

KW-2449 to T315I-mutated BCR/ABL, Aurora kinase inhibition, which was indicated by cell-cycle distribution in TCC-Y/sr, could contribute to the release of IM resistance. On the other hand, whereas IM showed $G_1$ arrest and ABL inhibition in wt-BCR/ABL cells, it had limited activity both in cell cycle and cell signaling in T315I-mutated BCR/ABL cells. These data indicated that the inhibition of wt- and T315I-mutated BCR/ABL kinase by KW-2449 at lower concentrations showed limited effects on cell viability, whereas the additional inhibitory effects on Aurora kinase by KW-2449 at higher concentrations modulated the survival and proliferation of the IM-resistant leukemia cells. These multifunctional action mechanisms, as well as the order of potency against various kinases, which were involved in oncogenic addiction and drug-resistance, would contribute to overcome the IM resistance.

It has been reported that potent and selective Aurora kinase inhibitors show remarkable growth inhibition of a variety of cancer cells in vitro, although several severe adverse events such as hematopoietic toxicity have been observed in the early-phase clinical trials. However, our results suggest that the additive and/or simultaneous inhibition of Aurora kinase at a lower potency than mainly targeted kinases might contribute to increase the growth inhibitory effects on cancer cells without severe adverse effects.

In conclusion, targeted inhibition of FLT3 kinase with KW-2449 induced the potent growth inhibition of leukemia cells transformed by the constitutive activation of FLT3 kinase. KW-2449 also showed growth inhibitory effects against FLT3 leukemia by its Aurora kinase inhibition. In addition, simultaneous inhibition of T315I-mutated BCR/ABL and Aurora kinases by KW-2449 also induced the growth inhibition of IM-resistant leukemia cells. Currently, KW-2449 is being investigated in a phase 1/2 study in patients with relapsed or refractory AML (NCT00779480). The present results, nevertheless, provide an important insight into clinical investigations for the treatment of patients with BCR/ABL-positive leukemia acquiring the IM resistance, including the T315I-mutation.

## Acknowledgments

The authors thank H. Kosugi for collecting clinical samples and S. Yamaji, E. Koshimura, M. Asano, and K. Higuchi for technical assistance.

This work was supported by the National Institute of Biomedical Innovation, Ministry of Health, Labor and Welfare, Ministry of Education, Culture, Sports, Science and Technology on the Scientific Research and the 21st Century COE Program Integrated Molecular Medicine for Neuronal and Neoplastic Disorders, Japan.

## Authorship

Contribution: Y. Shiotsu designed experiments; screened chemical libraries; performed cell-based assay, Western blot, and animal studies; analyzed data; generated figures; and wrote the manuscript; H.K. designed experiments; performed Western blot, colony assay, animal studies, and quantitative real-time RT-PCR; analyzed data; generated figures; and wrote the manuscript; Y.I. collected clinical samples and performed Western blot and FCM; R.T. performed animal studies, quantitative real-time RT-PCR, and pathologic analysis; M.S. performed FCM analysis and Western blot; H.U. screened chemical libraries; K.I. performed Western blot and animal studies; Y. Mori performed colony assay; K.O. collected clinical samples and performed animal studies and quantitative real-time RT-PCR; Y. Minami performed cell cycle analysis; A.A. performed animal studies; H.M. analyzed the LC/MS/MS; T.A. and S.A. provided input into experiment design; Y.K. provided input into chemical synthesis; Y. Sato established imatinib-resistant cell lines; and T.N. designed experiments and wrote the manuscript.

Conflict-of-interest disclosure: Y. Shiotsu, M.S., H.U., K.I., H.M., T.A., Y.K., and S.A. are employed by Kyowa Hakko Kirin Co Ltd. H.K. has a consultancy with Kyowa Hakko Kirin Co Ltd.

Correspondence: Yukimasa Shiotsu, Fuji Research Park, Kyowa Hakko Kirin, 1188 Shimotogari, Nagaizumi-cho, Sunto-gun, Shizuoka 411-8731, Japan; e-mail: yukimasa.shiotsu@kyowa-kirin.co.jp.

## References

1. Krause DS, Van Etten RA. Tyrosine kinases as targets for cancer therapy. *N Engl J Med.* 2005; 353:172-187.
2. Chalandon Y, Schwaller J. Targeting mutated protein tyrosine kinases and their signaling pathways in hematologic malignancies. *Haematologica.* 2005;90:949-968.
3. Druker BJ, Guilhot F, O'Brien SG, et al. Five-year follow-up of patients receiving imatinib for chronic myeloid leukemia. *N Engl J Med.* 2006;355:2408-2417.
4. Yanada M, Takeuchi J, Sugiura I, et al. High complete remission rate and promising outcome by combination of imatinib and chemotherapy for newly diagnosed BCR-ABL-positive acute lymphoblastic leukemia: a phase II study by the Japan Adult Leukemia Study Group. *J Clin Oncol.* 2006;24:460-466.
5. Stirewalt DL, Radich JP. The role of FLT3 in haematopoietic malignancies. *Nat Rev Cancer.* 2003;3:650-665.
6. Gilliland DG, Griffin JD. The roles of FLT3 in hematopoiesis and leukemia. *Blood.* 2002;100: 1532-1542.
7. Nakao M, Yokota S, Iwai T, et al. Internal tandem duplication of the flt3 gene found in acute myeloid leukemia. *Leukemia.* 1996;10:1911-1918.
8. Yamamoto Y, Kiyoi H, Nakano Y, et al. Activating mutation of D835 within the activation loop of FLT3 in human hematologic malignancies. *Blood.* 2001;97:2434-2439.
9. Kiyoi H, Yanada M, Ozekia K. Clinical significance of FLT3 in leukemia. *Int J Hematol.* 82:85-92.
10. Ozeki K, Kiyoi H, Hirose Y, et al. Biologic and clinical significance of the FLT3 transcript level in acute myeloid leukemia. *Blood.* 2004;103:1901-1908.
11. Gale RE, Hills R, Kottaridis PD, et al. No evidence that FLT3 status should be considered as an indicator for transplantation in acute myeloid leukemia (AML): an analysis of 1135 patients, excluding acute promyelocytic leukemia, from the UK MRC AML10 and 12 trials. *Blood.* 2005;106: 3658-3665.
12. Sternberg DW, Licht JD. Therapeutic intervention in leukemias that express the activated fms-like tyrosine kinase 3 (FLT3): opportunities and challenges. *Curr Opin Hematol.* 2005;12:7-13.
13. Stone RM, DeAngelo DJ, Klimek V, et al. Patients with acute myeloid leukemia and an activating mutation in FLT3 respond to a small-molecule FLT3 tyrosine kinase inhibitor, PKC412. *Blood.* 2005;105:54-60.
14. Fiedler W, Serve H, Döhner H, et al. A phase 1 study of SU11248 in the treatment of patients with refractory or resistant acute myeloid leukemia (AML) or not amenable to conventional therapy for the disease. *Blood.* 2005;105:986-993.
15. Knapper S, Burnett AK, Littlewood T, et al. A phase 2 trial of the FLT3 inhibitor lestaurtinib (CEP701) as first line treatment for older patients with acute myeloid leukemia not considered fit for intensive chemotherapy. *Blood.* 2006;108:3262-3270.
16. DeAngelo DJ, Stone RM, Heaney ML, et al. Phase 1 clinical results with tandutinib (MLN518), a novel FLT3 antagonist, in patients with acute myelogenous leukemia or high-risk myelodysplastic syndrome: safety, pharmacokinetics, and pharmacodynamics. *Blood.* 2006;108:3674-3681.
17. Knapper S. FLT3 inhibition in acute myeloid leukaemia. *Br J Haematol.* 2007;138:687-699.
18. Levis M, Pham R, Smith BD, Small D. In vitro studies of a FLT3 inhibitor combined with chemotherapy: sequence of administration is important to achieve synergistic cytotoxic effects. *Blood.* 2004;104:1145-1150.
19. Yee KW, Schittenhelm M, O'Farrell AM, et al. Synergistic effect of SU11248 with cytarabine or daunorubicin on FLT3 ITD-positive leukemic cells. *Blood.* 2004;104:4202-4209.
20. Kiyoi H, Naoe T. Biology, clinical relevance, and molecularly targeted therapy in acute leukemia

with FLT3 mutation. *Int J Hematol.* 2006;83:301-308.

21. Speck NA, Gilliland DG. Core-binding factors in haematopoiesis and leukaemia. *Nat Rev Cancer.* 2002;2:502-513.
22. Frohling S, Scholl C, Gilliland DG, Levine RL. Genetics of myeloid malignancies: pathogenetic and clinical implications. *J Clin Oncol.* 2005;23:6285-6295.
23. Renneville A, Roumier C, Biggio V, et al. Cooperating gene mutations in acute myeloid leukemia: a review of the literature. *Leukemia.* 2008;22:915-931.
24. Thomasson MH, Xiang Z, Walgren R, et al. Somatic mutations and germline sequence variants in the expressed tyrosine kinase genes of patients with de novo acute myeloid leukemia. *Blood.* 2008;111:4797-4808.
25. Loriaux MC, Levine RL, Tyner JW, et al. High-throughput sequence analysis of the tyrosine kinome in acute myeloid leukemia. *Blood.* 111: 4788-4796.
26. Zheng R, Levis M, Piloto O, et al. FLT3 ligand causes autocrine signaling in acute myeloid leukemia cells. *Blood.* 2004;103:267-274.
27. Kano Y, Akutsu M, Tsunoda S, et al. In vitro cytotoxic effects of a tyrosine kinase inhibitor STI571 in combination with commonly used antileukemic agents. *Blood.* 2001;97:1999-2007.
28. Minami Y, Yamamoto K, Kiyoi H, Ueda R, Saito H, Naoe T. Different antiapoptotic pathways between wild-type and mutated FLT3: insights into therapeutic targets in leukemia. *Blood.* 2003;102: 2969-2975.
29. Osumi K, Fukui T, Kiyoi H, et al. Rapid screening of leukemia fusion transcripts in acute leukemia by real-time PCR. *Leuk Lymphoma.* 2002;43: 2291-2299.
30. Ninomiya M, Abe A, Katsumi A, et al Homing, proliferation and survival sites of human leukemia cells in vivo in immunodeficient mice. *Leukemia.* 2007;21:136-142.
31. Kiyoi H, Shiotsu Y, Ozeki K, et al. A novel FLT3 inhibitor FI-700 selectively suppresses the growth of leukemia cells with FLT3 mutations. *Clin Cancer Res.* 2007;13:4575-4582.
32. Levis M, Brown P, Smith BD, et al. Plasma inhibitory activity (PIA): a pharmacodynamic assay reveals insights into the basis for cytotoxic response to FLT3 inhibitors. *Blood.* 2006;108:3477-3483.
33. Weisberg E, Boulton C, Kelly LM, et al. Inhibition of mutant FLT3 receptors in leukemia cells by the small molecule tyrosine kinase inhibitor PKC412. *Cancer Cell.* 2002;1:433-443.
34. Harrington EA, Bebbington D, Moore J, et al. VX-680, a potent and selective small-molecule inhibitor of the Aurora kinases, suppresses tumor growth in vivo. *Nat Med.* 2004;10:262-267.
35. Apperley JF. Part I: mechanisms of resistance to imatinib in chronic myeloid leukaemia. *Lancet Oncol.* 2007;8:1018-1029.
36. Quintas-Cardama A, Kantarjian H, Cortes J. Flying under the radar: the new wave of BCR-ABL inhibitors. *Nat Rev Drug Discov.* 2007;6:834-848.

bjh research paper

# CMC-544 (inotuzumab ozogamicin) shows less effect on multidrug resistant cells: analyses in cell lines and cells from patients with B-cell chronic lymphocytic leukaemia and lymphoma

**Akihiro Takeshita,[1,2] Kaori Shinjo,[2] Nozomi Yamakage,[1] Takaaki Ono,[2] Isao Hirano,[2] Hirotaka Matsui,[2] Kazuyuki Shigeno,[2] Satoki Nakamura,[2] Tadasu Tobita,[3] Masato Maekawa,[1] Kazunori Ohnishi,[2] Yoshikazu Sugimoto,[4] Hitoshi Kiyoi,[5] Tomoki Naoe[5] and Ryuzo Ohno[6]**

*[1]Laboratory and [2]Internal Medicine, Hamamatsu University School of Medicine, Handayama, Higashiku, Hamamatsu, [3]Yaizu Shimin Hospital, Dohara, Yaizu, [4]Graduate School of Pharmaceutical Science, Keio University, Shibakoen, Minatoku, Tokyo, [5]Haematology and Oncology, Nagoya University School of Medicine, Tsurumai, Showaku, and [6]Aichi Cancer Centre, Kanokoden, Chikusaku, Nagoya, Japan*

Received 26 December 2008; accepted for publication 17 March 2009

Correspondence: Akihiro Takeshita, Laboratory and Internal Medicine, Hamamatsu University School of Medicine, 1-20-1 Handayama, Higashiku, Hamamatsu 431-3192, Japan.
E-mail: akihirot@hama-med.ac.jp

## Summary

The effect of CMC-544, a calicheamicin-conjugated anti-CD22 monoclonal antibody, was analysed in relation to CD22 and P-glycoprotein (P-gp) in B-cell chronic lymphocytic leukaemia (CLL) and non-Hodgkin lymphoma (NHL) *in vitro*. The cell lines used were CD22-positive parental Daudi and Raji, and their P-gp positive sublines, Daudi/MDR and Raji/MDR. Cells obtained from 19 patients with B-cell CLL or NHL were also used. The effect of CMC-544 was analysed by viable cell count, morphology, annexin-V staining, and cell cycle distribution. A dose-dependent, selective cytotoxic effect of CMC-544 was observed in cell lines that expressed CD22. CMC-544 was not effective on Daudi/MDR and Raji/MDR cells compared with their parental cells. The MDR modifiers, PSC833 and MS209, restored the cytotoxic effect of CMC-544 in P-gp-expressing sublines. In clinical samples, the cytotoxic effect of CMC-544 was inversely related to the amount of P-gp ($P = 0{\cdot}003$), and to intracellular rhodamine-123 accumulation ($P < 0{\cdot}001$). On the other hand, the effect positively correlated with the amount of CD22 ($P = 0{\cdot}010$). The effect of CMC-544 depends on the levels of CD22 and P-gp. Our findings will help to predict the clinical effectiveness of this drug on these B-cell malignancies, suggesting a beneficial effect with combined use of CMC-544 and MDR modifiers.

**Keywords:** CMC-544, monoclonal antibody, CD22, P-glycoprotein, calicheamicin.

Rituximab in combination with chemotherapy has been used to treat various subtypes of B cell malignancies including chronic lymphocytic leukaemia (B-CLL) and non-Hodgkin lymphoma (B-NHL) (Hiddemann *et al*, 2006; Montserrat *et al*, 2006; Coiffier, 2007; Fanale & Younes, 2007). However, a considerable number of patients are refractory to treatment with rituximab and relapse after demonstrating an initial response. Several prognostic factors have been reported (Auer *et al*, 2007; Bonavida, 2007). The refractory nature to treatment may be partly attributed to the development of multidrug resistance (MDR), involving a series of events by which malignant cells become resistant to several structurally unrelated agents for B cell malignancies (Svoboda-Beusan *et al*, 2000; Andreadis *et al*, 2007). To overcome this resistance, several new agents have been developed (Hiddemann *et al*, 2006). Among these, CMC-544 has been introduced as a promising agent for the treatment of refractory and resistant cases.

CMC-544, inotuzumab ozogamicin, is a conjugate of N-acetyl γ-calicheamicin dimethyl hydrazide (NAc γ-calicheamicin DMH) and a recombinant humanized antibody ($IgG_4$) directed against the CD22 antigen (DiJoseph *et al*, 2004, 2006, 2007). Calicheamicin, a very potent anti-tumour antibiotic agent, binds to the minor groove of DNA in a sequence-specific manner, and breaks double-stranded DNA by abstracting specific hydrogen atoms, which may be the initial step in cell damage (Zein *et al*, 1988).

Gemtuzumab ozogamicin (GO), another immunoconjugate of NAc γ-calicheamicin DMH, is targeted to the human CD33 antigen and has been widely utilized for the treatment of acute

First published online 20 April 2009
doi:10.1111/j.1365-2141.2009.07701.x

 

myeloid leukaemia (AML) (Larson *et al*, 2005). However, the clinical outcome after treatment with GO was negatively associated with drug resistance in AML (Naito *et al*, 2000; Matsui *et al*, 2002; Walter *et al*, 2007). These effects, which are closely related to the expression of CD33 and P-glycoprotein (P-gp), have been reported by several investigators, including our laboratory (Naito *et al*, 2000; Matsui *et al*, 2002; Takeshita *et al*, 2005).

Thus, P-gp may also play a role in clinical resistance to CMC-544. If calicheamicin were pumped out by P-gp in the same manner as GO, CMC-544 would be less effective on B-CLL and NHL cells that express P-gp. This study investigated the cytotoxic effect of CMC-544 in relation to P-gp on cell lines and malignant cells from patients with B-CLL and NHL. Furthermore, other factors, such as level of CD22 and internalisation, were analysed regarding the effect of CMC-544.

## Materials and methods

### *Cells*

CD22-positive cell lines used were Epstein–Barr virus (EBV)-positive human lymphoma cell lines, Daudi and Raji, and their mdr-1 DNA-transduced Daudi and Raji sublines, Daudi/MDR and Raji/MDR (Sugimoto *et al*, 1997). $1{\cdot}0 \times 10^7$ and $6{\cdot}3 \times 10^5$ copies of *ABCB1* mRNA (*ABCB1/GAPDH* was 1·261 and 0·078 respectively) were detectable in Daudi/MDR and Raji/MDR respectively, by quantitative polymerase chain reaction (Yajima *et al*, 1998), but it was not detectable in Daudi and Raji cells. Intracellular accumulation of rhodamine-123 (Rh123) shows a large amount of P-gp in Daudi/MDR and Raji/MDR cells (Takeshita *et al*, 2003). After the cells were cultured for 72 h with increasing concentrations of CMC-544, 50% inhibitory concentration values (IC50s) were measured by the dye elusion test with propidium iodide (PI) staining. IC50s of CMC-544 were 7 and 13 ng/ml calicheamicin in Daudi and Raji cells respectively. In contrast, IC50s in Daudi and Raji MDR sublines were 560 and 380 ng/ml respectively. The IC50s of Daudi/MDR and Raji/MDR cells were around 80 and 30 times higher than Daudi and Raji cells respectively. *ABCC1* mRNA and *LRP1* mRNA were not detectable. The CD22-negative cell lines used were a human chronic myeloid leukaemia cell line, K562 (Riken Cell Bank, Tsukuba, Japan); a T-cell leukaemia cell line, Jurkat (Riken Cell Bank); a human acute promyelocytic leukaemia cell line, NB4 (kindly provided by Dr M Lanotte, Hospital Saint-Louis, Paris, France).

These cell lines were cultured in RPMI 1640 medium, supplemented with L-glutamine (2 mmol/l), antibiotics and 10% foetal calf serum (FCS; Gibco BRL, Grand Island, NY, USA), (10% FCS-RPMI) at 37°C. Vincristine sulphate (4 ng/ml) was added every 3 weeks to the culture medium of Daudi/MDR and Raji/MDR cell lines (Sugimoto *et al*, 1997).

After informed consent, peripheral blood cells were collected from five patients with B-CLL, and lymphoma cells were separated from lymph nodes of 14 patients with NHL. The cells were purified by Ficoll–Hypaque centrifugation (Phamacia, Uppsala, Sweden).

### *Flow cytometric analyses for CD-phenotype and immunoglobulin on cells*

In all analyses, cells were stained by phycoerythrin-cyanin 5.1 (PC5)-conjugated anti-CD45 monoclonal antibody (mAb) (Becton Dickinson Immunocytometry Systems, San Jose, CA, USA) and gated by the pattern of side scatter (SCC) and CD45 expression (CD45-gating) with an Epics XL flow cytometer (Beckman Coulter, Fullerton, CA, USA) (Matsui *et al*, 2002). Cells were additionally stained by fluorescein isothiocyanate (FITC)- or phycoerythrin (PE)-conjugated anti-CD2, CD3, CD4, CD5, CD7, CD8, CD10, CD11c, CD16, CD19, CD20, CD22, CD23, CD25, CD30, CD34, CD56, κ-chain or λ-chain mAbs (Becton Dickinson Immunocytometry Systems) according to the manufacturer's instructions. We examined the ratio of κ- to λ-chain expressing cells in the CD45-gated group and only used samples in which the ratio was 20 times or more.

Specifically, for the detection of CD22, cells were stained with a FITC-labelled anti-CD22 mAb, HIB22 (Becton Dickinson Immunocytometry Systems). Ten thousand events were counted by flow cytometry. The dissociation of mean fluorescence intensity (MFI) of cells that reacted with anti-CD22 mAb and that of the subclass-matched mAb was determined.

In the analysis for internalisation of CMC-544, cells were pre-incubated with CMC-544 (5 ng/ml calichemicin DMH) at 37°C for 1 h, and washed three times. Then the cells were stained with FITC-labelled anti-human IgG mAb (Becton Dickinson Immunocytometry Systems) and incubated with CMC-544-free medium for 2 h. MFI of cells after the incubation was compared to that of before. The ratio (%) of MFI was used as a marker of the internalisation.

### *Flow cytometric analysis for P-glycoprotein*

For P-gp analysis, cells were reacted with biotinylated MRK16 (Fab') mouse mAb or with a subclass-matched control mAb and then stained with streptavidin- FITC (Becton Dikinson Immunocytometry Systems) as previously described (Takeshita *et al*, 2005). The degree of dissociation between the fluorescence intensity of cells that reacted with MRK16 and the respective subclass-matched mAb was analysed by the channel-by-channel subtraction method (Beckman Coulter). The cell count in each channel of the control histogram was subtracted from the cell count in the corresponding channel of the test histogram. The differences for all channels were totalled to calculate P-gp presence (%) (Müller *et al*, 1994; Naito *et al*, 2000; Takeshita *et al*, 2005).

P-gp function was determined by measuring intracellular Rh123 accumulation and its enhancement by MDR modifiers, such as PSC833 (Novartis Pharma, Basel, Swizerland) or MS209 (Mitsui Phamaceuticals, Chiba, Japan), as previously

described (Nakanishi *et al*, 1997; Merlin *et al*, 1998; Matsui *et al*, 2002; Takeshita *et al*, 2005).

### *Humanized anti-CD22 monoclonal antibody and CMC-544*

The humanized $IgG_4$ anti-CD22 mAb, G5/44, and NAc-γ-calicheamicin DMH-conjugated to the humanized $IgG_4$ anti-CD22 mAb, CMC-544, were kindly provided by Wyeth Research (Collegeville, PA, USA) (DiJoseph *et al*, 2004). The calicheamicin-conjugated humanized $IgG_4$ anti-CD33 mAb, GO, and unconjugated NAc-γ-calicheamicin DMH were also provided. After the cells were incubated with various concentrations of CMC-544 or G5/44 at 37°C for 2 h, they were washed and resuspended in 10% FCS-RPMI and prepared for subsequent analysis.

### *Cell cycle distribution analysis*

Cells were incubated with CMC-544 containing 5–100 ng/ml calicheamicin for 2 h and washed. The cell cycle distribution was analysed after incubation in CMC-544-free medium for 72 h. Cells were gently suspended in 1 ml hypotonic fluorochrome solution containing PI. The cell cycle distribution was quantified by flow cytometry (Naito *et al*, 2000; Takeshita *et al*, 2005). These experiments were also analysed in the presence of 50–100 μmol/l Z-VAD-FMK (Calbiochem, Darmstadt, Germany), a caspase inhibitor, to study the apoptotic mechanisms of CMC-544. If samples from patients were contaminated with 5% or more of non-B cells by examining cell-surface antigens described before, malignant cells were sorted by the CD45-gating with a FACS Aria (Becton Dickinson, Franklin Lakes, NJ, USA) prior to cell cycle analysis.

### *Morphological analysis by a video-microscopic technique*

Cells ($1 \times 10^5$ cells/ml) were plated in a glass-bottomed dish (MatTec Corporation, Ashland, MA, USA) and incubated with CMC-544 containing 10 ng/ml calicheamicin for 2 h before washing. After 24- and 48-h incubations at 37°C in CMC-544 free medium, cells were observed under an inverted Normarski microscope (Axiovert 35; Zeiss, Oberkochen, Germany) as described previously (Naito *et al*, 2000).

### *Dye exclusion test with PI staining*

After incubation of cells with CMC-544 or G5/44 for the indicated periods of time, cells were stained with 0·1 μg/ml PI solution and counted under the microscope (Takeshita *et al*, 2005). Viable cell counts were calculated as follows: (viable cell counts) = (total cell counts) − (PI stained cell counts). The viable cell count following incubation with CMC-544 was compared with that following incubation with G5/44.

### *The process of CMC-544-induced cell death*

Cell death was quantitated using an Apocyto® kit containing Annexin V-Azami-Green and PI (Karasawa *et al*, 2003). Viable cells were not stained by either agent (Annexin−PI−), while early apoptotic cells were stained by Annexin V-Azami-Green (Annexin+PI−), and late apoptotic cells were stained by both agents (Annexin+PI+). Cells damaged via a non-apoptotic mechanism were stained only by PI (Annexin−PI+).

### *In vitro effect of CMC-544 in the presence of MDR modifiers*

Cells were pre-incubated in the presence or absence of 2 μmol/l PSC833 or 5 μmol/l MS209 in a humidified $CO_2$ incubator at 37°C for 1 h. The cells were then incubated with or without CMC-544 containing 5–100 ng/ml calicheamicin in the presence or absence of 2 μmol/l PSC833 or 5 μmol/l MS209 at 37°C for 2 h. After incubation, the cells were washed three times to remove unbound CMC-544. They were then re-incubated in CMC-544-free medium at 37°C for 24–48 h. The viability of cells just after incubation with CMC-544 was 99·6% by the dye exclusion test, which was carried out as described in our previous reports on GO (Naito *et al*, 2000; Matsui *et al*, 2002; Takeshita *et al*, 2005).

## Results

### *CD22 expression on cell lines*

CD22, which was expressed on Daudi and Raji cells, was equally expressed on Daudi/MDR and Raji/MDR cells respectively (Fig 1A). However, it was not expressed on Jurkat, K562 nor NB4 cells. The amount of CD22 was unchanged after a 2-h incubation with the experimental concentration of MDR modifiers, 2 μmol/l PSC833 or 5 μmol/l MS209 (Fig 1A).

### *Cell growth assay of P-gp negative cells*

The viable cell counts of Daudi and Raji cells decreased in a time- and dose-dependent manner at 48 h after incubation with CMC-544 containing 5–100 ng/ml calicheamicin (Fig 1B). However, the change was not observed in CD22 negative Jurkat or NB4 cells.

### *Cell growth of Daudi/MDR and Raji/MDR in the absence or presence of MDR modifiers, PSC833or MS209*

In the absence of PSC833 or MS209, even CMC-544 containing 100 ng/ml calicheamicin did not suppress the cell growth of Daudi/MDR and Raji/MDR cells. In the presence of 2 μmol/l PSC833 or 5 μmol/l MS209, CMC-544 recovered its cytotoxic effect and suppressed the cell growth in a dose-dependent manner (Fig 1C). Cells treated with only PSC833 or MS209 at the same concentrations did not show significant growth changes.


 

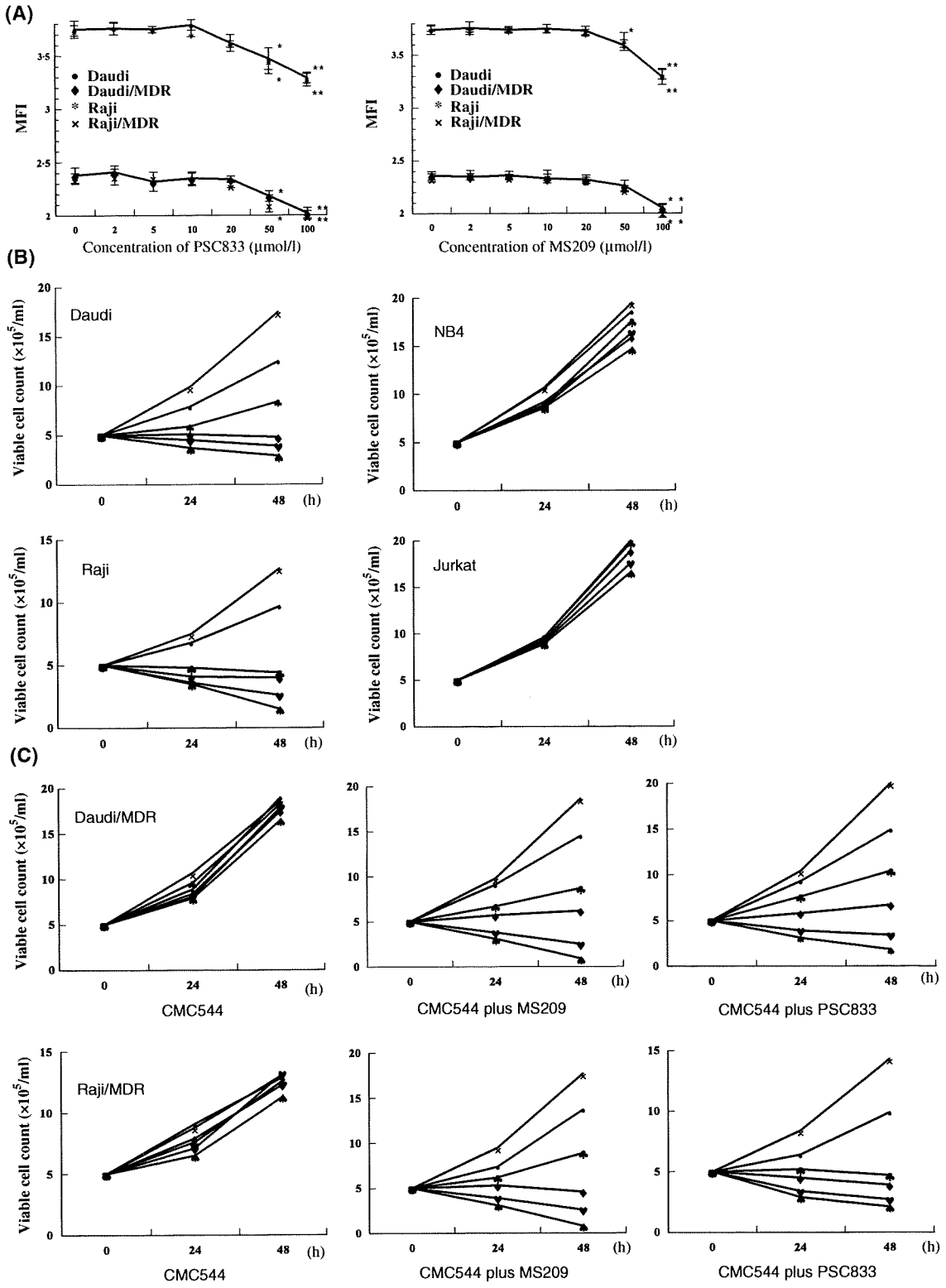


Fig 1. (A) Daudi (●) and Raji (*) cells and their MDR sublines, Daudi/MDR (◆) and Raji/MDR (x), were stained by FITC-labelled anti-CD22 mAb after a 2-h incubation with 0, 2, 5, 10, 20, 50, 100 μmol/l of PSC833 or MS209. CD22 level was not influenced by 0–20 μmol/l of PSC833 or MS209. (B) Cell growth of Daudi, Raji, Jurkat, and NB4 cells analysed by flow cytometry after incubation with G5/44 or various concentrations of CMC-544 for 48 h (x) G5/44, (●) 5 ng/ml, (♣) 10 ng/ml, (◆) 20 ng/ml, (♥) 50 ng/ml and (♠) 100 ng/ml calicheamicin. (C) Cell growth of Daudi/MDR and Raji/MDR cells analysed by flow cytometry at 48 h after incubation with CMC-544 containing 10 ng/ml calicheamicin in the absence or presence of 5 μmol/l MS209 or 2 μmol/l PSC833.

### *Cell cycle distribution of CD22-positive and negative cells*

Cell cycle distribution patterns of Daudi and Raji cells at 0-, 12-, 24-, 48-, 72-h after incubation with CMC-544 containing 5 ng/ml calicheamicin were analysed (Fig 2A). Daudi and Raji cells arrested at the G2/M phase before the hypodiploid portion increased. In the presence of 50–100 μmol/l Z-VAD-fmk, while G2/M arrest was apparent, G0/G1 and G2/M phases were restored thereafter without a following increase in the hypodiploid portion. In Jurkat, NB4 and K562 cells, no effect was observed after the incubation of CMC-544 (data not shown). G5/44 did not affect the cell cycle distribution.

### *Cell cycle distribution of Daudi/MDR and Raji/MDR sublines*

CMC-544 had a dose-dependent effect on the cell cycle distribution of Daudi and Raji cells. The pattern was not changed in either Daudi/MDR or Raji/MDR cells incubated with G5/44 or CMC-544 containing 5–100 ng/ml calicheamicin (Fig 2B). However, in the presence of 2 μmol/l PSC833 (bottom line in Fig 2B) or 5 μmol/l MS209 (data not shown), addition of CMC-544 recovered the effect and arrested the cell cycle in both cell lines at G2/M phase.

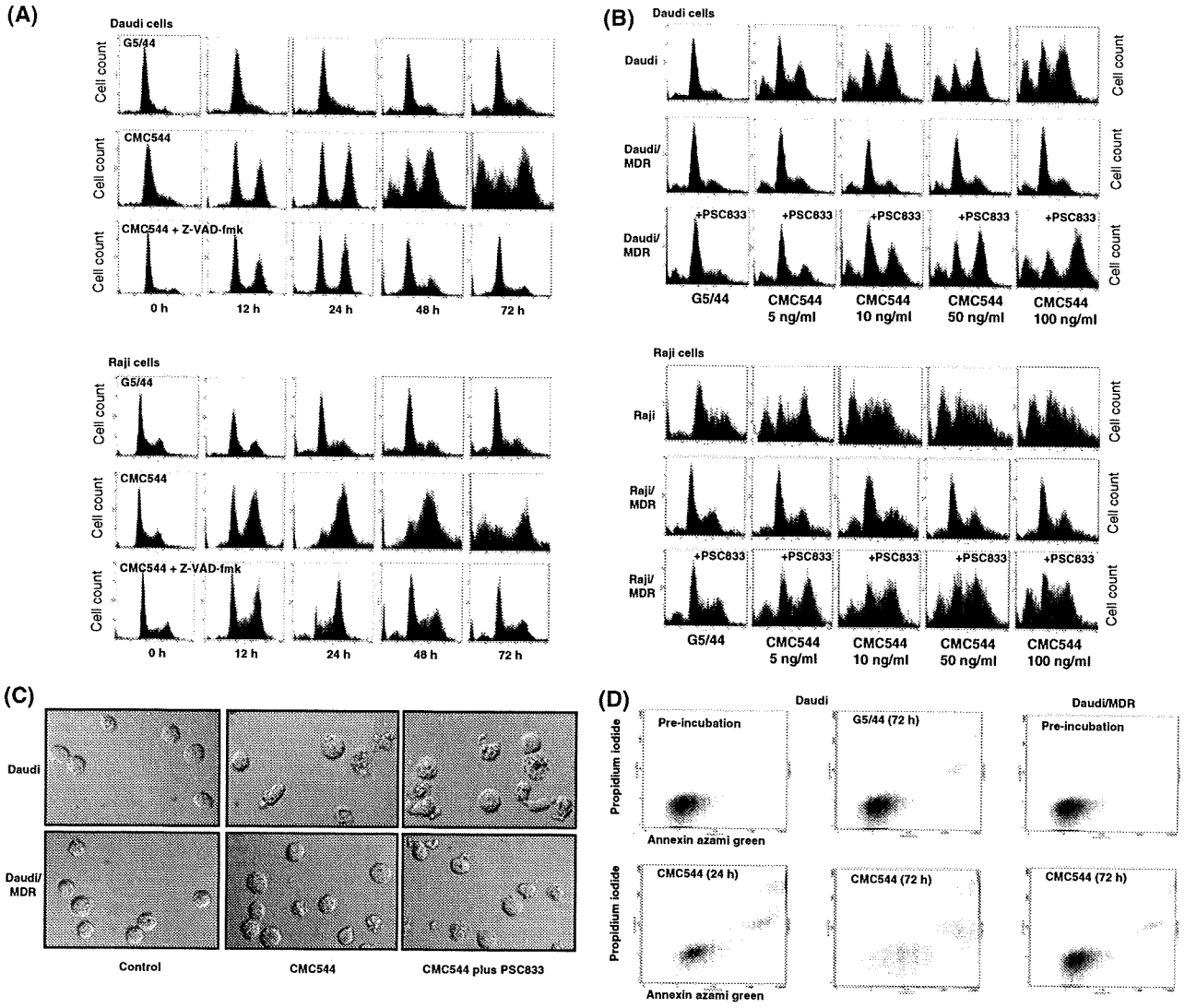


Fig 2. (A) Cell cycle distribution at 0, 12, 24, 48 and 72 h after incubation with G5/44 or CMC-544 with or without 100 μmol/l Z-VAD-fmk. (B) Cell cycle distribution of Daudi and Daudi/MDR cells, and Raji and Raji/MDR cells 48 h after incubation with G5/44 or CMC-544 containing 5, 10, 50 or 100 ng/ml calicheamicin in the absence or presence of 2 μmol/l PSC833. (C) Morphological changes of Daudi and Daudi/MDR cells were observed using a video-microscope. Daudi cells were incubated in medium containing CMC-544 with or without 2 μmol/l PSC833 for 24 h. Original magnification ×400. (D) Apoptotic mechanism of CMC-544 in the figures of Apocyto®. Daudi and Daudi/MDR cells were incubated in medium containing CMC-544 or G5/44, and were stained by PI (vertical lines) and Annexin-V Azami Green (horizontal lines).



 

*Morphological observation by a video-microscopic technique*

Daudi cells became enlarged after 24-h incubation with CMC-544 compared with the control cells incubated with G5/44 alone. Morphological changes of apoptosis, characterized by bleb formation and shrinkage of cells, were observed in 35% of the cells (Fig 2C). These morphological changes were rarely observed in the Daudi/MDR cells. CMC-544 recovered the effect in the presence of 2 μmol/l PSC833 (Fig 2C) or 5 μmol/l MS209 (data not shown).

*The process of CMC-544-induced cell death*

Apoptotic analyses of CMC-544 using an Apocyte® kit are summarized in Fig 2D. After incubation of Daudi cells with CMC-544 containing 10 ng/ml calicheamicin, Annexin−PI− cells decreased concomitantly with an increase of Annexin+PI− and Annexin+PI+ cells in a time dependent manner, while Annexin−PI+ cells did not significantly increase. However, Daudi/MDR cells were not changed significantly at 72 h after the incubation with CMC-544. G5/44 did not change the distributions significantly.

*The in vitro cytotoxic effect of CMC-544 in the samples from B-CLL and NHL cases*

The relationships among the *in vitro* effect of CMC-544, internalisation, CD22 and P-gp levels were investigated using cells from 19 patients with B-CLL and NHL. The characteristics and results of the cases are summarized in Table I. The *in vitro* effect of CMC-544 was significantly correlated with the amount of CD22 ($P = 0{\cdot}010$), but it was inversely correlated with the amount of P-gp ($P = 0{\cdot}003$) or the percentage increase of intracellular Rh123 level in the presence of PSC833 or MS209 ($P < 0{\cdot}001$) (Fig 3). Additionally, we determined internalisation level of CMC-544 by analysing CMC-544 conjugated fluorescence before and after the incubation of antibody-free medium for 2 h. The damping degree of the fluorescence was not related to cytotoxicity of CMC544, CD22 and P-gp level ($P = 0{\cdot}26$, $P = 0{\cdot}90$ and $P = 0{\cdot}89$ respectively) in the patient samples. Some of the cells that had low sensitivity for CMC544, despite low P-gp levels, had a relatively low CD22 level (Case 14) or low internalisation (Case 4).

## Discussion

Antibody-targeted chemotherapy is one of the most promising treatments for refractory or resistant haematological malignancies (Faderl *et al*, 2005; Cheson, 2006; Fanale & Younes, 2007; Taksin *et al*, 2007). For example, calicheamicin-conjugated antibodies have yielded informative results, and GO continues to provide encouraging clinical results. However, drug efflux mediated by P-gp leads to the development of drug resistance to GO, and inhibition of P-gp effectively increases GO-induced cytotoxicity *in vitro* (Naito *et al*, 2000; Matsui *et al*, 2002; Takeshita *et al*, 2005). In fact, P-gp is related to adverse clinical outcomes after GO-based therapy (Walter *et al*, 2007). Our present study suggests that CMC-544, a promising new drug for B-cell malignancies, is also affected by P-gp.

CD22-positive malignant cell lines, such as Daudi and Raji cells, were killed by CMC-544, while CD22-negative cell lines, such as NB4 and Jurkat cells, were not. Similar to GO (Naito *et al*, 2000), CMC-544 arrested the cell cycle at the G2/M phase and increased the hypodiploid portion in Daudi and Raji cells. In the presence of Z-VAD-fmk, while G2/M arrest was apparent, G0/G1 and G2/M phase were restored thereafter without a following increase in hypodiploid portion. The results indicate that the G2/M arrest by CMC544 is transient and a considerable number of cells might undergo apoptosis after release from G2/M arrest caused by the caspase. However, the proportion of cells moving to apoptosis via this pathway is still unclear. The caspase and its inhibitor may have a role in resistance to CMC-544, although they were not examined extensively in this study.

While several studies of CMC-544 have recently been published (DiJoseph *et al*, 2004, 2006, 2007), there is currently no published literature regarding CMC-544 in relation to P-gp. Our study suggested that the effect of CMC-544 may also be affected by P-gp. Using our newly established *MDR1* DNA-transduced Daudi and Raji sublines, we directly investigated the effect of CMC-544 on P-gp, an advantage over previously established drug-resistant cell lines that generally co-express other resistant mechanisms in addition to P-gp. Our results showed that CMC-544 had no effect on the P-gp expressing sublines compared with the parental cell lines, even though the former expressed sufficient levels of CD22. P-gp is a membrane glycoprotein that actively pumps cytotoxic agents out of cells and decreases the intracellular concentration of the agents, independently of their structure (Kartner *et al*, 1985). Therefore, if calicheamicin becomes detached from CMC-544 within the cell, it should be pumped out of the cell by P-gp. This hypothesis was endorsed by a combined use of CMC-544 and MDR modifiers. Both PSC833, a non-immunosuppressive analogue of cyclosporine, and MS209, a quinoline compound, are potent MDR-reversing drugs (Nakanishi *et al*, 1997; Merlin *et al*, 1998). These modifiers recovered the cytotoxic effect of CMC-544 in P-gp expressing sublines. The combination of CMC-544 and MDR modifiers may be an ideal therapeutic approach to treat P-gp-related resistant B-CLL and NHL. Haematologic and non-haematologic toxicities, which were observed in a clinical trial that utilized a combination of GO and MDR modifiers (Tsimberidou *et al*, 2003), might not be worsened in the case of CMC-544 because CD22 is expressed at lower levels in haematopoietic and non-haematopoietic immature cells than CD33 (Tedder *et al*, 1997).

Several resistant mechanisms in the treatment of B-cell malignancies have been reported, including alterations of intracellular cell death pathways, such as p53 and Bcl-2 family